

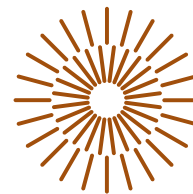


Master Thesis

Optimization of the thin-film composite membrane using various monomers in the aqueous phase

Study programme: N0723A270002 Textile Engineering
Author: **Vipin Kumar Veeramuthu**
Thesis Supervisors: doc. Fatma Yalcinkaya, MSc. Ph.D.
Institute of Mechatronics and Computer
Engineering

Liberec 2024



Master Thesis Assignment Form

Optimization of the thin-film composite membrane using various monomers in the aqueous phase

Name and surname: **Vipin Kumar Veeramuthu**
Identification number: T21000311
Study programme: N0723A270002 Textile Engineering
Assigning department: Department of Nonwovens and Nanofibrous materials
Academic year: 2022/2023

Rules for Elaboration:

1. Literature research on given topic
2. Current state of art for selected membrane technology
3. Membrane synthesis and design
4. Optimization and characterization of thin film membranes, and test for salt rejection
5. Evaluate the results and discussion
6. Conclude the research and discuss for the future prospective

Scope of Graphic Work: as required
Scope of Report: 40-60
Thesis Form: printed/electronic
Thesis Language: english

List of Specialised Literature:

- [1] Yalcinkaya, B., Yalcinkaya, F. and Chaloupek, J., 2017. Optimisation of thin film composite nanofiltration membranes based on laminated nanofibrous and nonwoven supporting material. *Desalination and Water Treatment*, 59, pp.19-30.
- [2] Shaari, N.Z.K., Sulaiman, N.A. and Abd Rahman, N., 2019. Thin film composite membranes: Preparation, characterization, and application towards copper ion removal. *Journal of Environmental Chemical Engineering*, 7(1), p.102845.
- [3] Lau, W.J., Ismail, A.F., Misdan, N. and Kassim, M.A., 2012. A recent progress in thin film composite membrane: A review. *Desalination*, 287, pp.190-199.
- [4] Lihong, W.A.N.G., Deling, L.I., Cheng, L., Zhang, L. and Huanlin, C.H.E.N., 2011. Preparation of thin film composite nanofiltration membrane by interfacial polymerization with 3, 5-diaminobenzoylpiperazine and trimesoyl chloride. *Chinese Journal of Chemical Engineering*, 19(2), pp.262-266.
- [5] Yalcinkaya, B., Yalcinkaya, F. and Chaloupek, J., 2016. Thin film nanofibrous composite membrane for dead-end seawater desalination. *Journal of Nanomaterials*, 2016.

Thesis Supervisors: doc. Fatma Yalcinkaya, MSc. Ph.D.
Institute of Mechatronics and Computer
Engineering

Date of Thesis Assignment: November 1, 2022

Date of Thesis Submission: January 8, 2024

doc. Ing. Vladimír Bajzík, Ph.D.
Dean

L.S.

prof. Ing. Jakub Wiener, Ph.D.
study programme guarantor

Liberec November 1, 2022

Declaration

I hereby certify, I, myself, have written my master thesis as an original and primary work using the literature listed below and consulting it with my thesis supervisor and my thesis counsellor.

I acknowledge that my master thesis is fully governed by Act No. 121/2000 Coll., the Copyright Act, in particular Article 60 – School Work.

I acknowledge that the Technical University of Liberec does not infringe my copyrights by using my master thesis for internal purposes of the Technical University of Liberec.

I am aware of my obligation to inform the Technical University of Liberec on having used or granted license to use the results of my master thesis; in such a case the Technical University of Liberec may require reimbursement of the costs incurred for creating the result up to their actual amount.

At the same time, I honestly declare that the text of the printed version of my master thesis is identical with the text of the electronic version uploaded into the IS/STAG.

I acknowledge that the Technical University of Liberec will make my master thesis public in accordance with paragraph 47b of Act No. 111/1998 Coll., on Higher Education Institutions and on Amendment to Other Acts (the Higher Education Act), as amended.

I am aware of the consequences which may under the Higher Education Act result from a breach of this declaration.

May 20, 2024

Vipin Kumar Veeramuthu

ACKNOWLEDGEMENT

First and foremost, I wish to extend my sincere gratitude to my supervisor, **doc. Fatma Yalcinkaya, Ph.D., M.Sc.**, for her unwavering encouragement, support, and guidance throughout my study, research, and experimentation. Most importantly, I am grateful for her motivation, which was instrumental in completing this thesis.

I would like to express my gratitude to the Department of **Nonwovens and Nanofibrous Materials (KNT)** and **Ing. Hana Musilová** for their great support and guidance throughout my studies.

ABSTRACT

This thesis presents an in-depth investigation into the optimization and performance evaluation of thin-film composite (TFC) membranes fabricated via interfacial polymerization, utilizing piperazine (PIP), m-phenylenediamine (MPD), and 1,3,5-Benzenetricarbonyl trichloride (TMC) as key monomers. The study aims to enhance the understanding of membrane-based filtration processes and improve the efficiency of water desalination and purification systems.

The PIP-TMC membrane demonstrated exceptional performance with a 97% rejection rate for divalent salts (MgSO_4) and a flux rate of 8.6 L/m²h. The MPD-TMC membrane, while achieving a 74% rejection rate for monovalent salts (NaCl), exhibited a lower flux rate of 0.42 L/m²h. The influence of pH variations in the feedwater on membrane performance was also examined, revealing that increased pH levels enhance rejection rates with minimal impact on flux.

Surface morphology analysis, contact angle measurements, and chemical composition analysis provided insights into the membranes structural and surface properties. The PIP-TMC membrane moderate hydrophilicity, indicated by its contact angle, contributed to its high permeability and fouling resistance. In contrast, the MPD-TMC membrane exhibit less hydrophilicity, reflected in its contact angle, suggested robust structural integrity and selective ion rejection.

The findings underscore the critical role of monomer selection and polymerization conditions in determining membrane properties and performance. The study concludes that optimizing TFC membranes for specific filtration applications can significantly improve their efficiency and effectiveness, paving the way for advancements in water treatment technologies.

Keywords:

Thin-film composite membranes, interfacial polymerization, water desalination, membrane optimization, filtration performance, surface morphology, contact angle measurement.

ABSTRAKT

Tato práce představuje hloubkový výzkum optimalizace a hodnocení výkonu tenkovrstvých kompozitních membrán (TFC) vyrobených pomocí mezifázové polymerizace s využitím piperazinu (PIP), m-fenylendiaminu (MPD) a 1,3,5-Benzenetrikarbonyltrichloridu (TMC) jako klíčových monomerů. Cílem studie je zlepšit porozumění filtračním procesům na bázi membrán a zlepšit účinnost systémů odsolování a čištění vody.

Membrána PIP-TMC prokázala výjimečný výkon s 97% mírou rejekce dvojmocných solí ($MgSO_4$) a průtokem 8,6 l/m²h. Membrána MPD-TMC sice dosáhla 74% míry rejekce monovalentních solí (NaCl), ale vykazovala nižší průtok 0,42 l/m²h. Byl také zkoumán vliv změn pH v přírodní vodě na výkonnost membrány, přičemž se ukázalo, že zvýšené hodnoty pH zvyšují míru rejekce s minimálním dopadem na průtok.

Analýza morfologie povrchu, měření kontaktního úhlu a analýza chemického složení umožnily získat informace o strukturálních a povrchových vlastnostech membrán.

Mírná hydrofilita membrány PIP-TMC, indikovaná jejím kontaktním úhlem, přispěla k její vysoké propustnosti a odolnosti proti zanášení. Naproti tomu membrána MPD-TMC vykazovala menší hydrofilitu, která se odráží v jejím kontaktním úhlu, což naznačuje robustní strukturní integritu a selektivní odmítání iontů.

Tato zjištění zdůrazňují rozhodující úlohu výběru monomeru a polymeračních podmínek při určování vlastností a výkonu membrán. Studie dochází k závěru, že optimalizace TFC membrán pro specifické filtrační aplikace může významně zlepšit jejich účinnost a efektivitu, což otevírá cestu k pokroku v technologiích úpravy vody.

Klíčová slova:

Tenkovrstvé kompozitní membrány, mezifázová polymerace, odsolování vody, optimalizace membrán, filtrační výkon, morfologie povrchu, měření kontaktního úhlu.

TABLE OF CONTENTS

ACKNOWLEDGEMENT	5
ABSTRACT	6
ABSTRAKT	7
TABLE OF CONTENTS	8
LIST OF TABLES	10
LIST OF FIGURES	11
LIST OF EQUATION.....	12
LIST OF SYMBOLS	13
1. INTRODUCTION:.....	14
2. THEORETICAL PART:	17
2.1. Membrane Technology:.....	17
2.1.1. Structure of membrane:.....	17
2.1.2. Driving force:.....	19
2.1.3. Membrane fabrication:.....	21
2.1.4. Composite membranes:.....	22
2.2. Thin-film Composite (TFC) Membrane:.....	25
2.3. Membrane Modification Techniques:	26
2.4. Aqueous Phase Monomers:.....	27
2.4.1. Interfacial polymerization:.....	27
2.4.2. Solution polymerization:.....	27
2.5. Previous Research in Membrane Optimization:.....	28
3. SCOPE OF THIS THESIS:	30
4. EXPERIMENTAL PART:	31
4.1. Materials used:	31
4.2. Monomer selection and preparation:.....	32
4.3. Experimental Design:.....	32
4.4. Membrane Fabrication:	33
4.5. Characterization of membranes.....	34
4.5.1. Surface Morphology of Membrane:.....	34

4.5.2.	Contact angle:	34
4.5.3.	Chemical composition analysis:	35
4.6.	Filtration test:	35
5.	RESULTS AND DISCUSSION:	37
5.1.	Results and discussion of filtration test and characterization of PIP-TMC membrane:	37
5.1.1.	Filtration test:	37
5.1.2.	Effect of pH in the feed of filtration test.....	39
5.1.3.	Double testing on one sample:	42
5.1.4.	Surface morphology analysis:.....	44
5.1.5.	Contact angle:	47
5.1.6.	Chemical Composition Analysis:.....	50
5.2.	Results and discussion of filtration test and characterization of MPD-TMC membrane: 51	
5.2.1.	Filtration test:	51
5.2.2.	Effect of pH in the feed of filtration test:.....	53
5.2.3.	Surface morphology analysis:.....	55
5.2.4.	Contact angle:	58
5.2.5.	Chemical Composition Analysis:.....	61
6.	CONCLUSION:	62
7.	REFERENCE:	63

LIST OF TABLES

Table 1: Driving force and their respective separation process.....	19
Table 2: List of materials used in this work.	31
Table 3: List of PIP-TMC membranes and their preparation condition.	37
Table 4: Comparison of flux and rejection of PIP-TMC membranes	37
Table 5: List of PIP-TMC membranes and their preparation condition for different pH feed.....	39
Table 6: Comparison of flux and rejection of feeds with different pH on PIP-TMC membranes	40
Table 7: The best sample of PIP-TMC was chosen for double testing and its preparation condition.	42
Table 8: comparison flux and rejection of chosen for double testing.	42
Table 9: list of PIP-TMC membranes for SEM analysis.....	44
Table 10: PIP-TMC sample list and preparation condition for contact angle measurement.....	47
Table 11: Average contact angle of PIP-TMC sample in different solution.	47
Table 12: Contact angle images of PIP-TMC membranes.	48
Table 13: List of MPD-TMC membranes and their preparation condition.	51
Table 14: Comparison of flux and rejection of MPD-TMC membranes	52
Table 15: List of MPD-TMC membranes and their preparation condition for different pH feed.	53
Table 16: Comparison of flux and rejection of feeds with different pH on MPD-TMC membranes.	53
Table 17: List of MPD-TMC membranes for SEM analysis.....	55
Table 18: MPD-TMC sample list and preparation condition for contact angle measurement.	58
Table 19: Average contact angle of MPD-TMC sample in different solution.....	58
Table 20: images of contact angle measurement on MPD-TMC membranes.....	59

LIST OF FIGURES

Figure 1: Cumulative installed Desalination capacities and year-on-year increase [2].	14
Figure 2: Source of feed water for global desalination capacity [2].	15
Figure 3: Schematic drawing of the membrane separation process.	17
Figure 4: Structure of symmetric membranes.	18
Figure 5: pressure-driven separation with filtration spectrum.	20
Figure 6: Schematic drawing of dip coating method [14].	22
Figure 7: polyamide formed with PIP-TMC by IP [22].	23
Figure 8: polyamide formed with MPD-TMC by polymerization [23].	24
Figure 9: Schematic drawing of the Interfacial polymerization (IP) process flow.	24
Figure 10: structure of Thin-film Composite (TFC) Membrane.	25
Figure 11: A graph of the number of publications about Membrane distillation, with a respective year, appeared in the Science Direct journal each year [37].	28
Figure 12: Schematic structure of prepared Thin-film nanofibrous composite (TFNC) membrane.	32
Figure 13: Schematic drawing of Membrane Fabrication process.	33
Figure 14: Krüss Drop Shape Analyser (DS4).	34
Figure 15: Thermo Scientific™ Nicolet iZ10.	35
Figure 16: Schematic drawing of dead-end filtration process.	36
Figure 17: Graph of flux and rejection of PIP-TMC membranes	38
Figure 18: Graph of flux and rejection on different pH feed with PIP-TMC membranes	40
Figure 19: Graph of flux and rejection of chosen sample for double testing	43
Figure 20: SEM images of PT1.	45
Figure 21: SEM images of PT2.	45

Figure 22: SEM images of PT3.	46
Figure 23: FT-IR of PIP-TMC based PA membrane.	50
Figure 24: Graph of flux and rejection of MPD-TMC membranes.	52
Figure 25: Graph of flux and rejection on Different pH feed with MPD-TMC membranes.	54
Figure 26: SEM images of MT1-S.	56
Figure 27: SEM images of MT2-S.	56
Figure 28: SEM images of MT3-S.	57
Figure 29: SEM images of MT4-S.	57
Figure 30: FT-IR of MPD-TMC based PA membrane.	61

LIST OF EQUATION

Equation 1: Formula for flux rate measuring.	36
Equation 2: Formula for calculating rejection.	36

LIST OF SYMBOLS

TFC	Thin-film composite
TFNC	Thin-film nanofibrous composite
PIP	Piperazine
MPD	m-Phenylenediamine
TMC	1,3,5-Benzenetricarbonyl trichloride
TEA	Triethylamine
NaOH	Sodium hydroxide
SDS	Sodium dodecyl sulphate
HCL	Hydrochloric acid
NaCl	Sodium chloride
MgSO ₄	Magnesium sulfate
IP	Interfacial polymerization
W/V	Weight divided volume
SEM	Scanning electron microscopy
PA	Scanning electron microscopy
FT-IR	Fourier-transform infrared spectroscopy
RO	Reverse osmosis
FO	Forward osmosis
NF	Nanofiltration
MF	Microfiltration
UF	Ultrafiltration
MD	Membrane distillation
GS	Gas Separation
MED	Multi-effect distillation
ppm	Parts per million
MSF	Multi-stage flash

1. INTRODUCTION:

Water is an essential component for the functioning of life on Earth. It is one of the primary things that makes Earth suitable for living. From the name universal solvent, we can understand how unique, functional, and essential it is. Our human body comprises 70% water, which is required for critical functions like metabolic activities and transporting nutrients and gases to all body parts. However, consuming contaminated or salty water can lead to severe health issues.

The Earth's 71% surface is covered by seas and oceans, which hold 96.5% of the total volume of water on Earth. A tiny portion of 1.7% of water lies in groundwater and 1.7% in glaciers[1]. This clarifies that most water on earth is salty and cannot be used for agriculture, industrial purposes, or drinking. A desalination process is mandatory to make seawater usable.

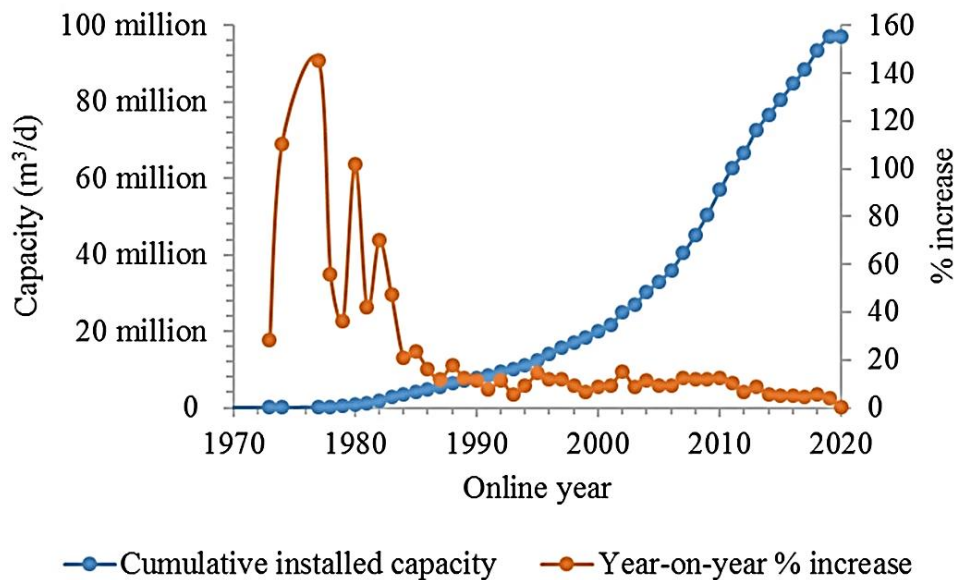


Figure 1: Cumulative installed Desalination capacities and year-on-year increase [2].

Figure 1 shows that the global desalination capacity across the global level has increased because of the increasing demand for fresh water. From the first multi-effect distillation (MED) plant in

1930 to the first multi-stage flash (MSF) distillation plant in 1957 to the first Reverse Osmosis (RO) plant in 1965, desalination technologies had seen a significant upturn since 1928 when they first started to appear in many of the world's water-stressed cities [2].

Growing population and demand for freshwater leads to finding better conditions (energy savings, cost savings, and ecological footprint reduction) for freshwater production, especially in membrane-based water desalination technologies like Reverse Osmosis (RO). Desalting seawater at a reasonable cost has become more appealing as a substitute for traditional municipal water supply methods. This explains why, since 2010, the number and size of desalination plants worldwide have increased at an average annual rate of roughly 6.8% or an addition of approximately 4.6 million m³/day of production capacity yearly. One hundred fifty-five new desalination plants were contracted and installed globally between 2019 and 2020, adding 5.2 million m³/day of installed capacity[2–4].

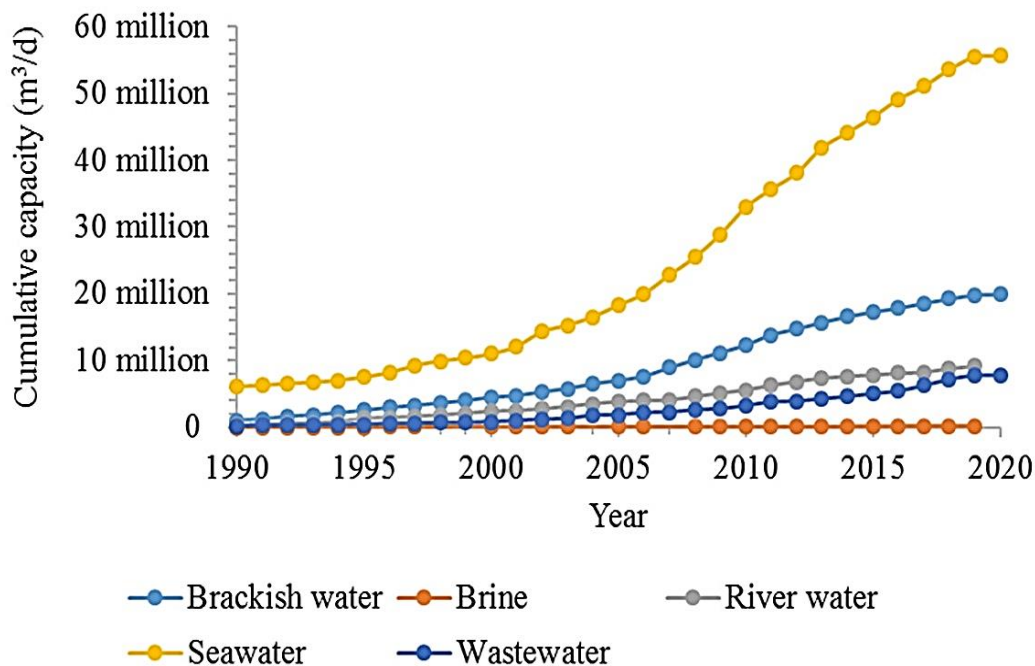


Figure 2: Source of feed water for global desalination capacity [2].

The primary source of desalination plants at a global level depends on seawater (Figure 2). RO technology is the leading desalination technology widely used to desalinate all types of feed waters out of all the technologies implemented yet to achieve global desalination capacity. Even though RO membrane-based desalination has given the best results until now, research on membrane technology is growing day by day because of the worldwide population increase, which demands more fresh water while at the same time requiring a cost-effective process. Membrane optimization is needed to prepare membranes with high flux and selectivity. Thin-film composite (TFC) membranes are the emerging ones in membrane technology and are well known for their selectivity and permeability. Using a nanofibrous layer as a substrate with the backing of nonwoven material to make a thin-film nanofibrous composite (TFNC) membrane gives promising results for future demand in the desalination process.

2. THEORETICAL PART:

2.1. Membrane Technology:

The membrane can be described as a thin sheet, layer or film that acts as a selective barrier between two phases: a liquid, gas or vapour. The membrane can be in the form of a solid, liquid or gel. It is considered a molecular sieve constructed as a film of more than one layered material with fine meshes or small pores to separate tiny particles and molecules, which allows certain substances to transit while retaining the others (Figure 3). Moreover, the transport between the feed and permeate can be active or passive. It can be made of natural or synthetic material and possibly neutral or charged. Membranes can be engineered to have distinct properties desired for specific separation processes [5, 6].

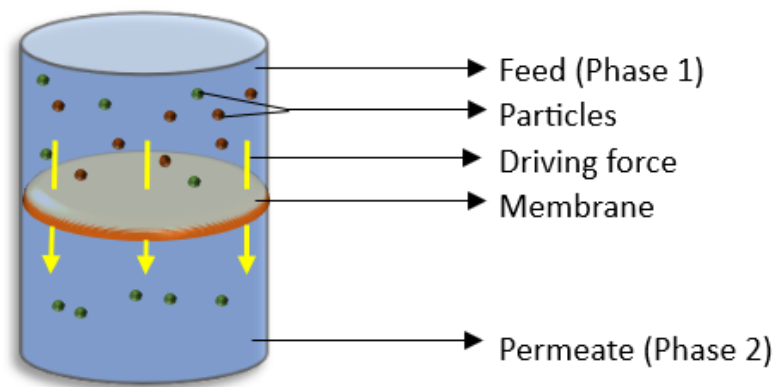


Figure 3: Schematic drawing of the membrane separation process.

2.1.1. Structure of membrane:

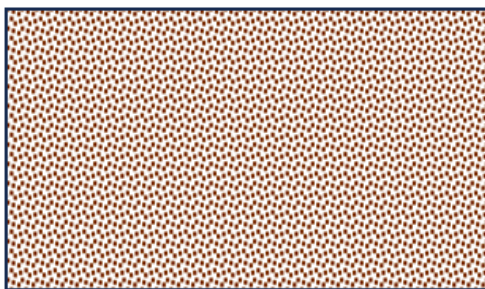
The membrane structure is one of the crucial parameters which determine the performance and efficiency of the separation process, as well as the durability of the membrane. The structure of the membrane can either be heterogeneous or homogenous and able to be produced as a thin or thick layer [7]. Permeability and flux are the two most vital Evaluation parameters in the separation process, which is controlled by the structure of the membrane. Precisely designed membrane

structures with controlled pore size and distribution can minimize energy usage during filtration and reduce the cost [8–10].

The structure of the Membrane plays a crucial role in preventing fouling, which can be achieved by modifying the membrane surface roughness and hydrophilicity [11, 12]. The membrane is classified into two main divisions based on the cross-sectional structure. Such as symmetric and asymmetric membranes.

2.1.1.1. Symmetric (Isotropic) membrane:

Symmetric membranes are homogeneous throughout their thickness and have a uniform distribution of pores with exact and identical pore sizes in all orientations. The preparation of symmetric membranes generally involves casting or forming a uniform layer of membrane material with consistent properties that are feasible to fabricate with desired and homogeneous pore sizes. These membranes are commonly adopted in Gas Separation (GS), Microfiltration (MF), and Ultrafiltration (UF) applications. Some common symmetric membranes are shown in Figure 4, such as Microporous and Non-porous dense membranes [8].



Microporous membrane



Non-porous dense membrane

Figure 4: Structure of symmetric membranes.

2.1.1.2. Asymmetric (anisotropic) membrane:

Asymmetric membranes are heterogeneously structured membranes with remarkable evolution in the filtration industry. These membranes comprise a highly dense top layer or film with 0.1 μm to 0.5 μm of thickness, supported by a porous sublayer. The membranes' pore size regulates the filtration process's characteristics, and the top layer regulates the mass transport through the membrane. Composite membranes are a well-known example of asymmetric membranes in which the top layer and the porous sublayer can also be prepared with different polymer materials with different properties. Each layer can be optimized individually as desired, i.e. Thin-film composite (TFC) membranes [13].

2.1.2. Driving force:

In the separation process, the driving force is an essential parameter for the factor or mechanism responsible for feed transport across the membrane. Understanding and manipulating the driving force is mandatory to optimize the performance and efficiency of membrane processes. The driving force can be either concentration Gradient, Pressure, Electric Potential, Temperature Gradient, or Chemical Potential Gradient between the feed and permeate in the filtration process. Table 1 gives the separation processes and their respective driving forces [8, 10].

Table 1: Driving force and their respective separation process.

Driving force	Membrane separation process
Pressure (ΔP)	Reverse osmosis (RO)
	Nanofiltration (NF)
	Microfiltration (MF)

Pressure (ΔP)	Ultrafiltration (UF)
Concentration (ΔC)	Dialysis
Electric charge (ΔE)	Electrodialysis
Thermal (ΔT)	Membrane distillation (MD)

2.1.2.1. Pressure-driven membranes:

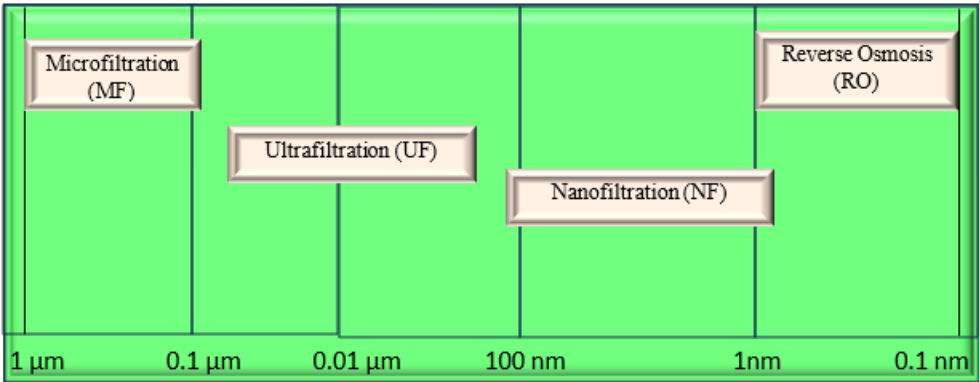


Figure 5: pressure-driven separation with filtration spectrum.

In the pressure-driven separation mechanism, the feed is transported through the membrane by a driving force of pressure difference in the feed and permeate. This process provides multiple advantages like ease of scalability and high efficiency with less energy consumption, capable of high-quality separation. This process is employed in wastewater treatment, food and beverage processing, pharmaceutical manufacturing, and various industries. Some of the common filtration processes that fall under this category are Reverse osmosis (RO), Nanofiltration (NF), Ultrafiltration (UF), and Microfiltration (MF)[14]. Figure 5 shows the filtration process and the respective particle size range that can be filtered.

2.1.3. Membrane fabrication:

Several membrane fabrication techniques are used today based on the desired properties required for the final separation process. Some of the preparation techniques are as follows

2.1.3.1. Phase inversion method:

One of the highly versatile methods to prepare membranes is the phase inversion method, where various morphologically structured membranes can be obtained [15]. Several phase inversion methods are employed in membrane fabrication, and all of them are based on the same principle of precipitation of polymers from homogeneous solutions. The precipitation is caused by the demixing of a solvent and a non-solvent exchange, which converts the solution from a liquid state to a porous solid state. Thermodynamics and phase inversion kinetics control the precipitation of polymer solution, which in turn influences the ultimate shape of produced membranes [16].

2.1.3.2. Stretching:

The stretching method of membrane fabrication was discovered in 1970. In this method, there will be no solvent, and the polymers are directly heated above their boiling point and prepared as a polymer solution, afterwards stretched to create a porous layer after being extruded into a thin-film. Stretched membranes are typically created through two sequential processes: 1) cold stretching, which creates micropores in the film, and 2) hot stretching, which modifies the membrane structure. Polymers with a high crystalline structure are preferred for this technique, which results in the formation of a strengthened and porous structure [17].

2.1.3.3. Track-etching:

The track-etching process comprises two distinct stages. Initially, a polymeric film is subjected to an intense bombardment of heavy ions, which cause disruption to the chemical bonds within the polymer and create linear patterns throughout the film. The second stage is chemical etching; the disrupted tracks are chemically etched to form hollow channels. The pore size distribution may be carefully controlled with track-etched membranes. Furthermore, there is a simplified relationship

between the morphology of the membrane and the properties of water transport since pore density and pore size are independent parameters with a broad range of control [18].

2.1.4. Composite membranes:

The development of composite membranes, which comprise a thin, dense layer supported by a porous sublayer, represents a pivotal advancement in the history of membrane technology. As each layer is manufactured using different techniques and materials, there is flexibility in optimising each layer separately. Moreover, materials such as elastomers, which are challenging or impossible to manufacture using traditional phase separation procedures, can be employed to prepare the top layer, which will be used as self-supporting membranes. Incorporating a support layer enables the fabrication of membranes exhibiting enhanced permeability, mechanical strength, selectivity and both chemical and thermal stabilities [5, 19].

2.1.4.1. Dip coating:

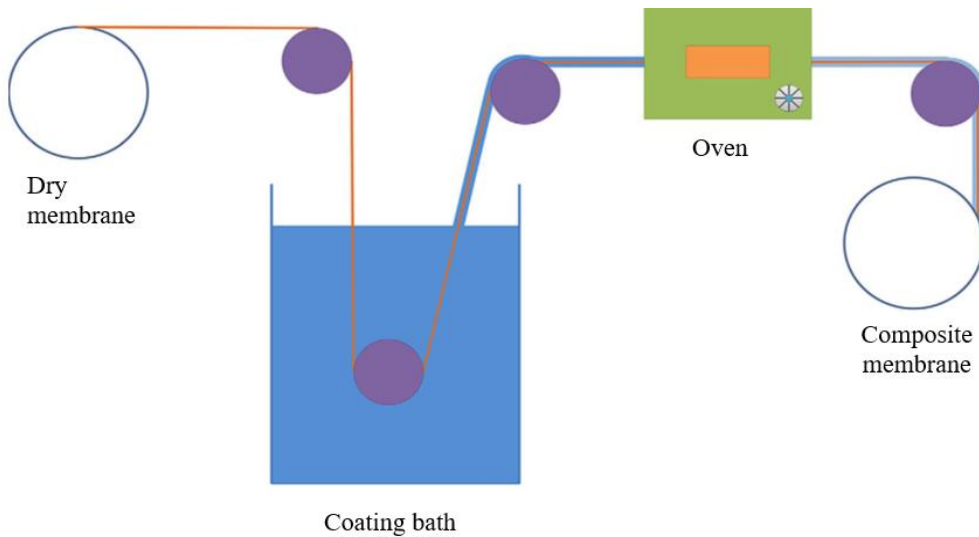


Figure 6: Schematic drawing of dip coating method [14].

A simple method for creating composite membranes with a thin, thick layer supported by a porous sublayer is dip coating. As shown in Figure 6, the process begins with the immersion of a porous substrate in a coating solution containing a prepolymer or polymer solution. After that, the coating solution is extracted from the support layer, leaving an adhesive coating solution layer on it. After that, the membrane is put in an oven to guarantee that the coated polymer on the porous layer is

crosslinked and the solvent evaporates. Crosslinking is necessary to ensure that the coated layer adheres firmly to the membrane surface because the coating lacks chemical and mechanical resilience when left alone [14].

2.1.4.2. Plasma polymerization:

Plasma polymerization is one of the techniques for directly depositing a thin, dense layer on the substrate. An electrical discharge at high frequencies ionizes an organic monomer gas, forming the plasma. Three steps are involved in plasma polymerization: firstly, the initiation stage, in which the collision of electrons and ions with gas monomers produces atoms and free radicals; secondly, the propagation stage, in which the polymeric chain is formed; and finally, the termination process, which is required to close the polymer chain. Plasma polymerization results in highly branched and cross-linked polymer films. This process is mainly used to modify the surface chemistry of membranes and add desired characteristics, like enhancing the hydrophilicity and antifouling properties of membrane [20, 21].

2.1.4.3. Interfacial polymerization (IP):

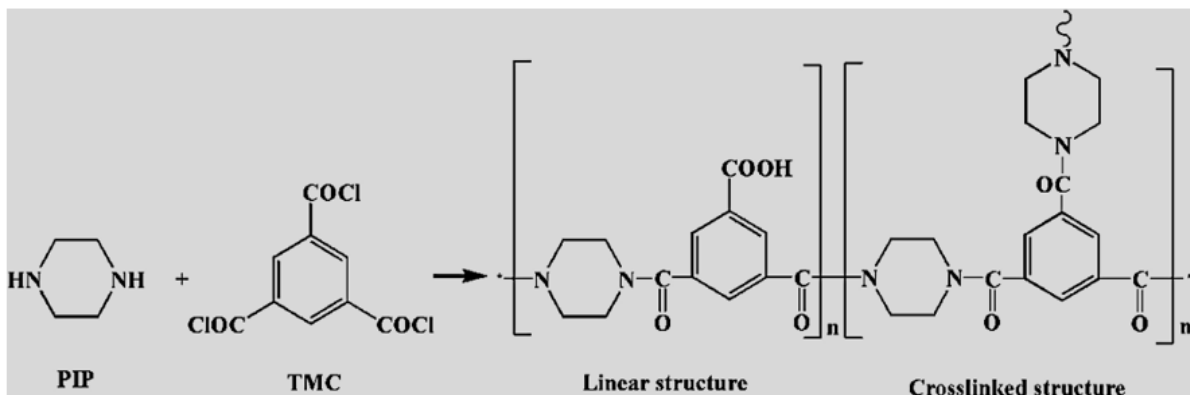


Figure 7: polyamide formed with PIP-TMC by IP [22].

MPD, PIP, and TMC are the monomers commonly used in the IP process. Figure 7 shows the structure of polyamide formed PIP-TMC by IP, and the polyamide structure formed with MPD-TMC is displayed in Figure 8.

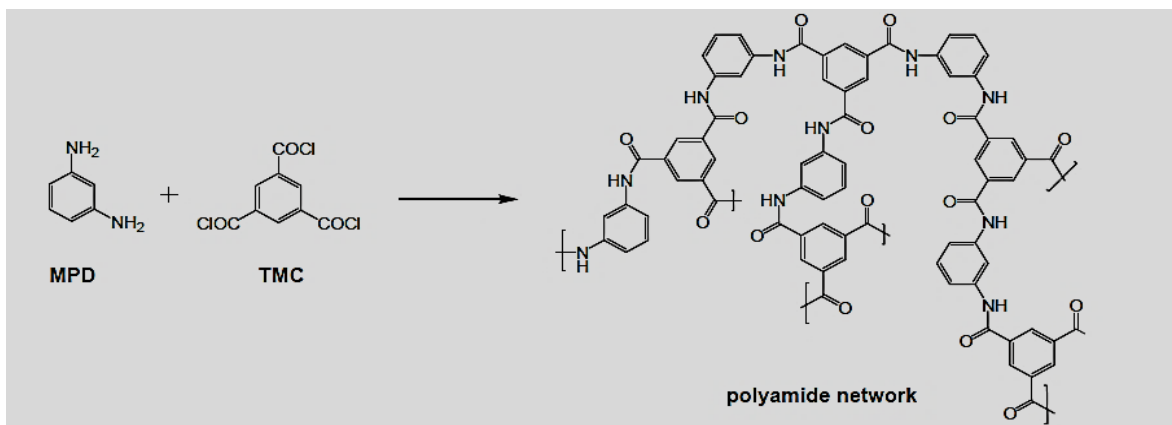


Figure 8: polyamide formed with MPD-TMC by polymerization [23].

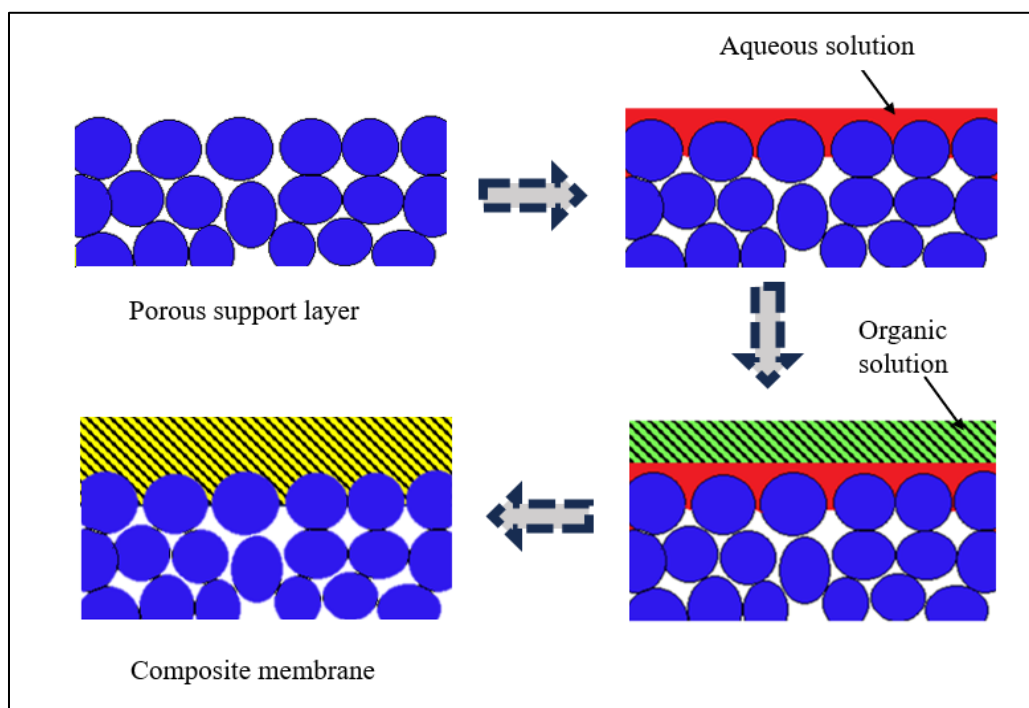


Figure 9: Schematic drawing of the Interfacial polymerization (IP) process flow.

IP is a method for creating a thin layer on a porous support by polymerization reaction. This reaction occurs between two monomers (amine-type and polyacyl chloride) that are highly reactive at the interface of two different immiscible solvents. As shown in Figure 9, a porous substrate is first immersed in the aqueous solution containing the amine-type monomer in a water solvent. Then, the substrate is immersed in the organic solution containing polyacyl chloride in hexane. These monomers react with each other and form a dense polymeric top layer on the porous

substrate. Heat is generally applied to finish the interfacial reaction and crosslink the pre-polymer or water-soluble monomer [24–27].

2.2. Thin-film Composite (TFC) Membrane:

Thin-film composite (TFC) membranes are a sort of composite membrane extensively employed in various separation procedures, most notably gas separation, water purification, and desalination. The fabrication process begins with the support material being saturated with an aqueous solution containing monomer A. Afterwards, an organic solution containing monomer B is introduced into the support. In the organic solvent, monomer A is typically far more soluble than monomer B is in the aqueous solution. As the polymer film forms, the interfacial polymerization slows down significantly. This happens due to the film's function in obstructing phase-to-phase contact, which causes a self-terminating reaction. These membranes comprise a porous substrate that supports a thin, dense polymeric active layer (Figure 10). The substrate offers mechanical support and makes it easier for fluids to pass through the membrane, while the active layer is for the selective separation of gases or solutes[27, 28].

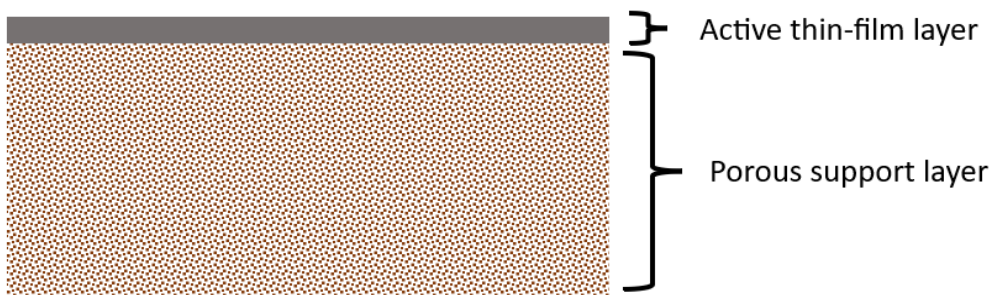


Figure 10: structure of Thin-film Composite (TFC) Membrane.

Despite being extensively utilized in membrane separation procedures, polymeric membranes have three primary drawbacks: poor thermal stability, membrane fouling, and a compromise between permeability and selectivity. However, TFC membranes can overcome these drawbacks, and that's why they are used widely in Reverse Osmosis (RO), Nanofiltration (NF), and Forward Osmosis (FO) processes[29, 30].

Their thin, dense active layer achieves high selectivity and flux, improving separation efficiency. Furthermore, TFC membranes can tolerate high pressures and challenging operating conditions because of the porous substrate's improved mechanical strength and stability. Membranes of this type have been broadly used in water treatment processes like desalination of seawater, wastewater treatment, and stream purification in industrial processes[8].

Scanning electron microscopy (SEM) is a popular method for analyzing the PA TFC membrane surface morphology. However, the film's uneven surface makes it difficult to determine its thickness accurately. High-resolution SEM has verified that the globular features on this rough surface are made of fully-aromatic polyamide films. When completely hydrated, these globular formations are filled with water[31].

2.3. Membrane Modification Techniques:

Various methods, such as surface modification through surface coating and surface grafting, have been developed for polymeric membrane modification. Different methods for performing surface grafting, including plasma treatment and UV irradiation. Among these techniques, surface grafting and surface coating are frequently employed to improve the anti-fouling characteristic and give the membrane a hydrophilic quality. However, these techniques only alter the membrane's external surface—internal pores remain unaltered, and membrane fabrication necessitates post-treatment. Blending inorganic fillers with polymeric membranes has improved the membranes' hydrophilicity, water flux, and antifouling properties[11, 32, 33].

Another method of modifying membranes is bulk modification, which involves blending hydrophilic additives into the membranes, such as incorporating nanoparticles using interfacial polymerization and radical polymerization. When preparing a composite membrane, blending with hydrophilic additives to change the membrane's characteristics without taking extra steps. The membrane can be tailored with different blend compositions to achieve the required membrane structure and yield different properties. Inorganic nanomaterials are incorporated into polymer matrices as nanofillers to improve membrane performance [32, 33].

2.4. Aqueous Phase Monomers:

Aqueous monomers are compounds soluble in water and used in various polymerization processes, particularly in interfacial and solution polymerization techniques. These monomers play a critical role in synthesizing polymers and copolymers for applications such as membrane fabrication, coatings, adhesives and biomedical materials. Aqueous phase monomers generally contain primary amine groups (NH_2) or other reactive functional groups. These monomers are dissolved in an aqueous solution to aid in the polymerization reaction at the interface between the organic and aqueous phases, frequently with the help of a catalyst or pH adjuster. Step-growth polymerization is when aqueous phase monomers react with organic phase monomers, usually diacid chlorides or diisocyanates dissolved in an organic solvent, to form polyamide or polyurea chains. Using aqueous phase monomers in membrane fabrication has various benefits, such as environmental friendliness, simple handling, and compatibility with aqueous-based processing techniques. Additionally, they make it possible to create high-performing TFC membranes with precisely controlled structure and characteristics. Several methods exist for polymerizing aqueous monomers [9, 34–36].

2.4.1. Interfacial polymerization:

Hydrophobic monomers react with aqueous monomers at the interface of two immiscible phases, usually an organic phase and an aqueous phase. This method is frequently applied to the fabrication of membranes [35].

2.4.2. Solution polymerization:

Using radical, anionic, or cationic initiation mechanisms, aqueous monomers are dissolved in water and then polymerized. This technique is frequently applied in hydrogel synthesis and copolymerization reactions, and it works well with monomers that dissolve in water [35].

2.5. Previous Research in Membrane Optimization:

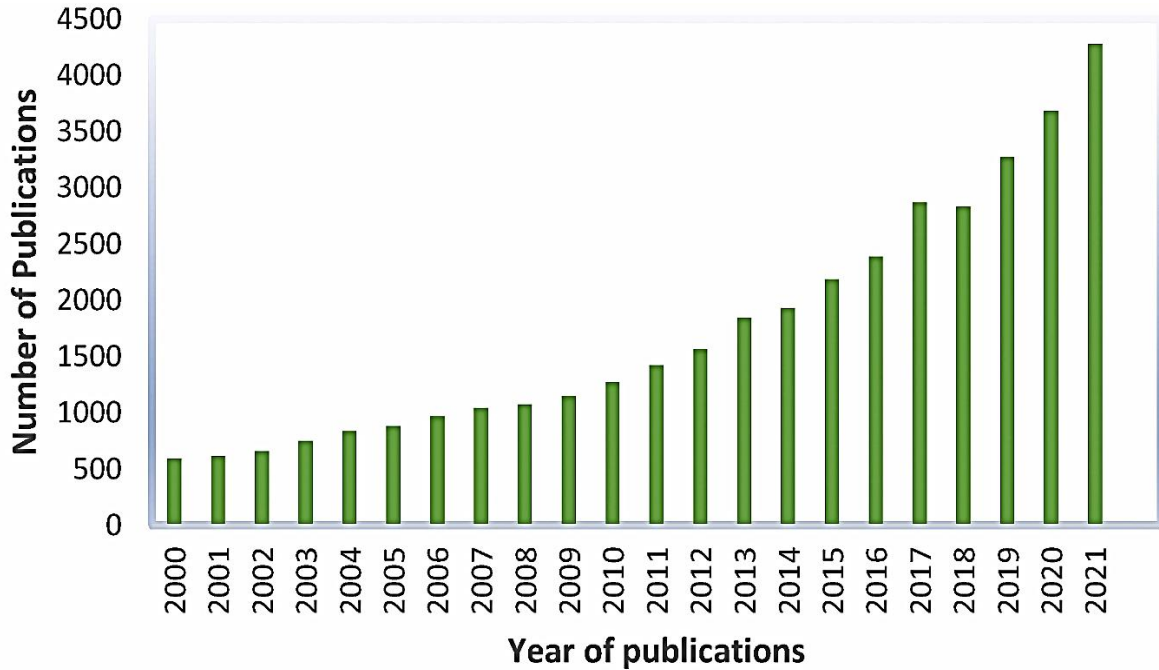


Figure 11: A graph of the number of publications about Membrane distillation, with a respective year, appeared in the Science Direct journal each year [37].

Because of their excellent heat stability and resistance to pH changes, polymer thin-film nanocomposite (TFC) membranes have recently drawn increased attention in wastewater treatment and purification processes. Figure 11 shows how drastically the increase in membrane distillation research is growing yearly.

Some of the closely related research to this thesis involves research conducted regarding membrane optimization, which involves modifying the concentration of the monomers, adding additives like surfactant and ionic liquids, exploring new materials and fabrication techniques to improve the performance and durability of membranes further, reducing fouling and scaling tendencies, and increasing energy efficiency [38–40]. Changing the reaction and curing conditions is one aspect of the optimization process that is involved [41].

According to research on monomer concentrations, changes in TMC and MPD concentrations significantly impact the hydrophilicity (-COOH) of the PA thin film. The structure of the PA films

also varies with reaction time, and the presence of third acyl chloride in TMC is crucial for high-performance membranes [42]. It has been observed that adding surfactant to the aqueous solution increases the wettability of the support material and makes the monomer penetrate through it. During polyamide synthesis, hydrogen chloride can be removed by adding Acylation catalysts, which speed up the reaction between two monomers [39, 40, 43]. Varying monomer types and concentrations directly impacted rejection and flux performance. The IP-produced MPD-TMC membranes exhibited rejection selectivity for monovalent (NaCl) salt ions due to the presence of an aromatic amine structure in the active barrier layer, which made the layer denser and more compact. The creation of a charged active barrier layer with pendant carboxylic acid groups in PIP-TMC membranes made by IP demonstrated rejection selectivity for divalent (MgSO_4) salt ions [44].

3. SCOPE OF THIS THESIS:

The main goal of this work is to prepare and optimize a thin-film polyamide (PA) membrane by Interfacial polymerization (IP) on the surface of a nanofibrous composite substrate. This results in the formation of a Thin-film nanofibrous composite (TFNC) membrane, which is used for desalination. The work also aims to understand the monomer effect on the selectivity of monovalent and divalent salts.

The primary goal of this thesis can be achieved by the following optimization process

- ❖ Optimization of concentration of monomer.
- ❖ Adding additives and surfactants in the monomer solution.
- ❖ Altering the curing procedures.
- ❖ Changing the pH of the feed solution.

Then characterize the prepared membrane by

- ❖ Surface morphology using Scanning Electron Microscopy.
- ❖ Composition analysis by Fourier-transform infrared spectroscopy (FT-IR).
- ❖ Hydrophilic and hydrophobic nature by water contact angle.
- ❖ Filtration test to determine the rejection and flux rate.

4. EXPERIMENTAL PART:

4.1. Materials used:

Table 2: List of materials used in this work.

Materials	From
Sodium chloride (NaCl)	Penta chemicals
Magnesium sulfate (MgSO ₄)	Penta chemicals
Piperazine (PIP)	Sigma-Aldrich
m-Phenylenediamine (MPD)	Sigma-Aldrich
1,3,5-Benzenetricarbonyl trichloride 98% (TMC)	Sigma-Aldrich
Triethylamine (TEA)	Sigma-Aldrich
Sodium hydroxide (NaOH)	Penta chemicals
Dodecyl sulfate sodium (SDS)	Sigma-Aldrich
n-Hexane	Penta chemicals
Hydrochloric acid (HCL)	Penta chemicals

A list of all monomers, chemicals and materials used in this thesis work is depicted in Table 2.

4.2. Monomer selection and preparation:

MPD, PIP, and TMC are the monomers most often used to fabricate TFC membranes using the IP technique, which makes them suitable for this optimization process. Even though many membranes have good rejection, research has been ongoing to find the most appropriate membrane for water filtration, achieving good rejection with a combination of permeability and flux at a low cost.

An organic solution is prepared by adding TMC to a preheated hexane at 50 °C. Various concentrations of TMC (0.2, 0.3, 0.45, and 0.6 % (w/v)) in the organic solution are prepared for the optimization process.

An aqueous solution dissolves the PIP/MPD monomer in distilled water. PIP solution prepared by mixing 2 % (w/v) of PIP with 4 % (w/v) of TEA and 1 % (w/v) of NaOH dissolved in the distilled water. Mixed all together using the magnetic stirrer till well mixed and visible clear. MPD solution prepared by mixing 2 % (w/v) of MPD with 2 % (w/v) of TEA and 0.2 % (w/v) of SDS dissolved in the distilled water and stirred using the magnetic stirrer till well mixed and visible clear.

4.3. Experimental Design:

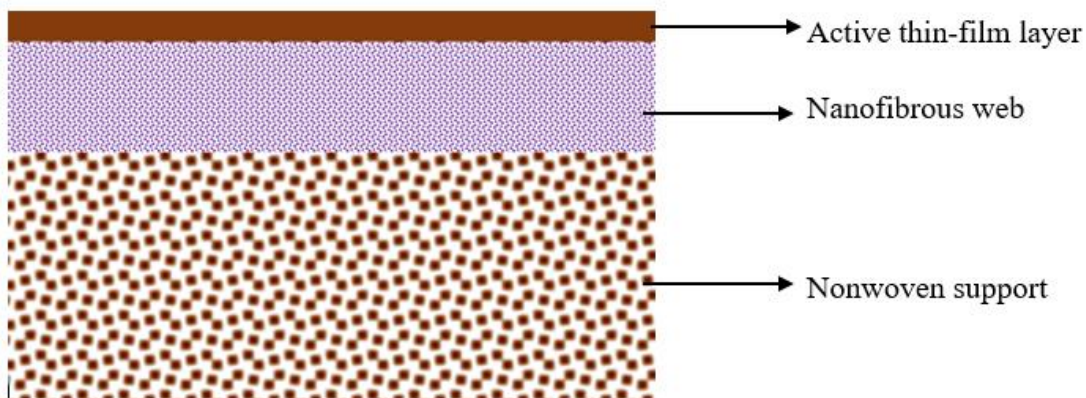


Figure 12: Schematic structure of prepared Thin-film nanofibrous composite (TFNC) membrane.

The main goal of the experiment is to fabricate and optimize an active thin-film layer on a composite substrate using various concentrations of monomer using the IP technique. The composite substrate is made by laminating a polyamide nanofibrous web with 1.5 GSM backed with a nonwoven material. In the experiment, an active thin-film layer is prepared on the composite substrate using the IP technique. Figure 12 shows a schematic drawing of the prepared TFNC membrane.

4.4. Membrane Fabrication:

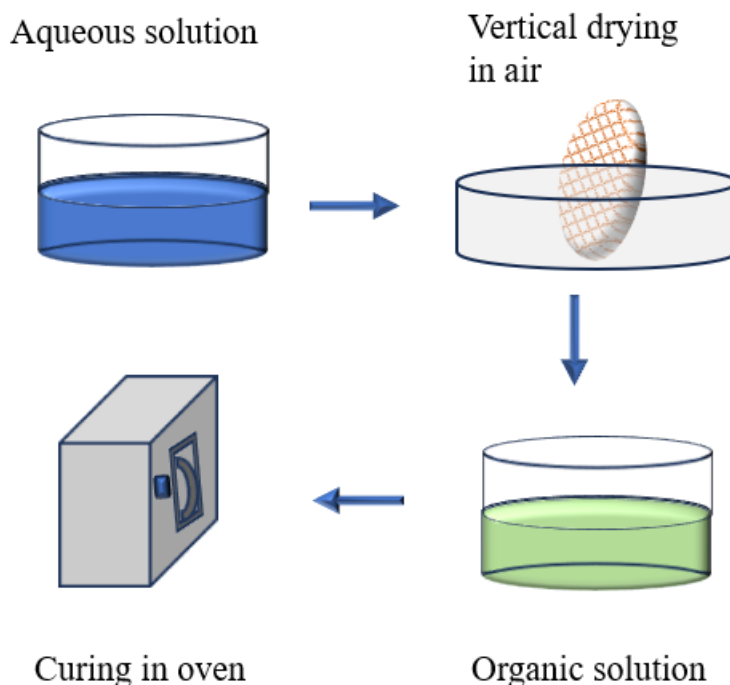


Figure 13: Schematic drawing of Membrane Fabrication process.

Fabrication of the active thin-film layer on the nanofibrous support was carried out in four stages, as shown in Figure 13. First, the composite substrate is immersed in the aqueous solution completely for 3 minutes, and in the second stage, the excess solution is removed by placing it vertically in a petri dish in the open air for 2 minutes and 30 seconds. The third stage is immersing

it in the organic solution bath for exactly 3 minutes, where the two monomers start to react, and the final stage of curing is applying heat of 100 °C for 10 minutes to cross-link. Membrane will be stored in distilled water after fabrication for at least 12 hours before the evaluation.

4.5. Characterization of membranes

4.5.1. Surface Morphology of Membrane:

The surface morphology, such as surface roughness, structure, and defects of the prepared active thin-film layer on the composite material, was analyzed by SEM using TESCAN VEGA (Brno, Czech Republic). The results were compared with the filtration results to determine the conclusion.

4.5.2. Contact angle:

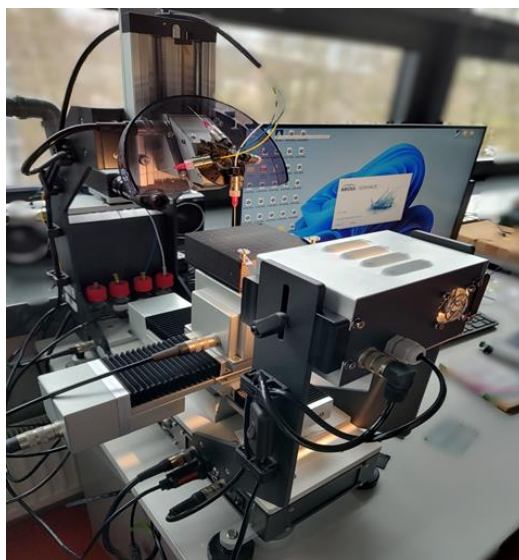


Figure 14:Krüss Drop Shape Analyser (DS4).

The prepared sample's contact angle was measured to determine its hydrophilic property, which determines its fouling behaviour, wetting characteristics, and interaction with feed. Three measurements were taken for each feed solution at room temperature. The measurements were carried out in the Krüss Drop Shape Analyser (DS4) (Figure 14) with all four types of feed solution used in the filtration test.

4.5.3. Chemical composition analysis:



Figure 15: Thermo Scientific™ Nicolet iZ10.

The thin-film membrane was produced without the composite support and analyzed using Fourier-transform infrared spectroscopy (FT-IR) with Thermo Scientific™ Nicolet iZ10 (Figure 15) to determine the chemical composition of the thin-film polyamide membrane.

4.6. Filtration test:

The filtration test was carried out in a dead-end filtration unit holding the 15 cm² of active filtration area from Millipore (XFUF04701). The salt feed solution of NaCl and MgSO₄ was prepared with 2000 ppm by dissolving in distilled water. The filtration tests were conducted by applying 4 bar of pressure with nitrogen gas, and before feeding with the feed, solution membranes were stabilized by passing distilled water through the membrane. The schematic drawing of the filtration test is shown in Figure 16. The flux of the membrane is measured using Equation 1 where A = the Area of filtration, *l* = volume of permeate collected and t = time taken to collect the permeate.

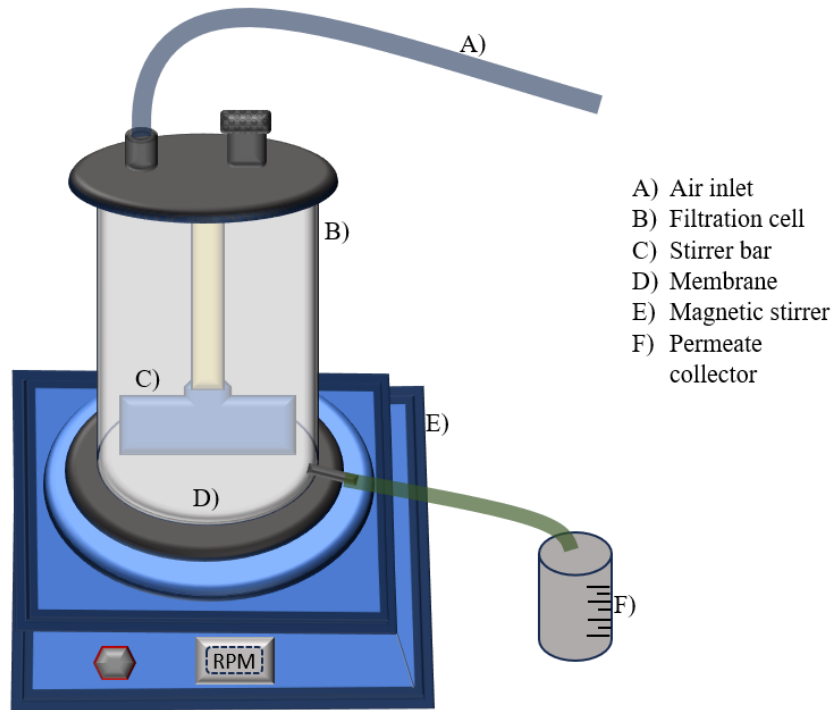


Figure 16: Schematic drawing of dead-end filtration process.

Equation 1: Formula for flux rate measuring.

$$\text{Flux} = \frac{l}{At} \text{ (L/m}^2\text{h)} \dots\dots\dots (1)$$

The rejection rate was evaluated using the conductivity meter from Thermo SCIENTIFIC (Orion STAR A112) with Equation 2, where C_f is the conductivity of the feed solution and C_p is the conductivity of the permeate solution.

Equation 2: Formula for calculating rejection.

$$\text{Rejection} = \frac{C_f - C_p}{C_f} \text{ (\%)} \dots\dots\dots (2)$$

5. RESULTS AND DISCUSSION:

5.1. Results and discussion of filtration test and characterization of PIP-TMC membrane:

5.1.1. Filtration test:

Table 3: List of PIP-TMC membranes and their preparation condition.

Sample name	Aqueous solution (S1) % w/v	Organic solution (S2) % w/v	Immersing time in S1	Drying at room temperature	Immersing time in S2	Curing
PT1	PIP 2% + TEA 4% + NaOH 1%	TMC 0.2 %	180 s	150 s	180 s	600 s at 100 °C
PT2	PIP 2% + TEA 4% + NaOH 1%	TMC 0.45 %	180 s	150 s	180 s	600 s at 100 °C
PT2-A	PIP 2% + TEA 4% + NaOH 1%	TMC 0.45 %	180 s	150 s	180 s	600 s at 100 °C

Table 4: Comparison of flux and rejection of PIP-TMC membranes

Sample name	Flux of distilled water (L/m ² h)	Type of salt feed	Flux of salt feed (L/m ² h)	Rejection (%)
PT1	26.6	MgSO ₄	10	91
PT2	16	MgSO ₄	8.6	97
PT2-A	31.6	NaCl	24	25

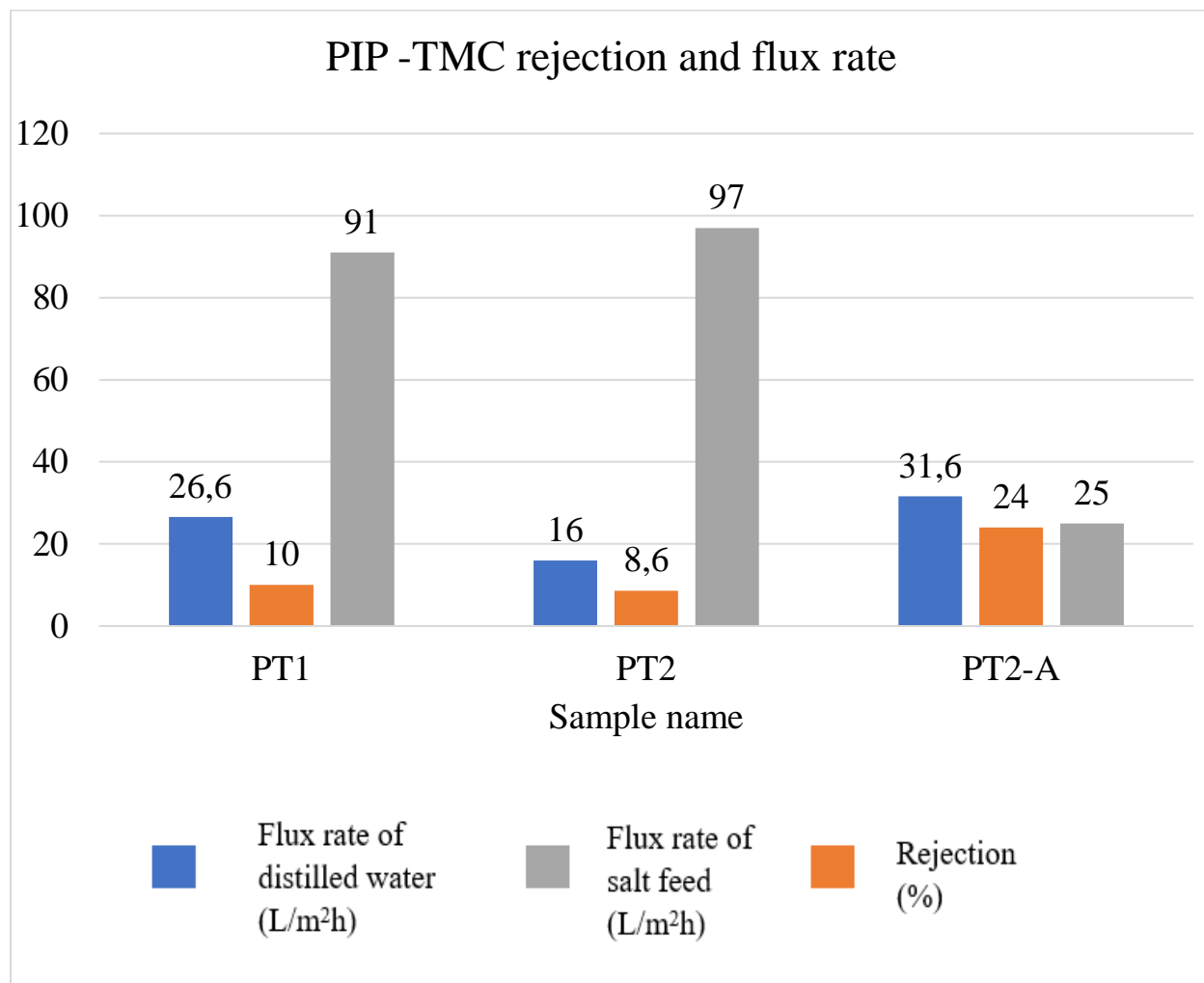


Figure 17: Graph of flux and rejection of PIP-TMC membranes

In the earlier experiments, it has been observed that the feeding of salt feed directly without stabilizing the membrane with distilled water shows low rejection. Then the membranes are first fed with distilled water till stable flow, and then the salt feed is introduced. This gives the best rejection rate. Table 3 gives out the preparation parameters for the PIP-TMC based membranes that are used for filtration tests to evaluate the filtration performance.

The obtained rejection and flux rates of distilled and feed water are depicted in Table 4. At the beginning of optimization, a high rejection of MgSO_4 divalent salt was observed with a low concentration of 0.2 % (w/v) of TMC. Increasing the concentration of TMC from 0.2 to 0.4 %

(w/v) in the organic solution resulted in a high rejection of 97 % but a slight decrease in flux. It has been observed that the flux rate decreases from time to time while testing. Previous studies showed that higher concentrations of TMC tend to enhance rejection rates due to increased cross-linking and membrane thickness but lead to reduced water flux. Conversely, decreasing TMC concentrations can improve water flux while decreasing the rejection capability[44, 45]

Then, the best-resulting concentration of TMC 0.45 % (w/v), which gives the highest rejection in divalent salt, was tested with the monovalent salt (NaCl) but, rejection was very low, 25%, with an increase in flux rate in comparison with the results of divalent salt rejection, which was shown in Figure 17. Due to the development of a charged active barrier layer containing pendant carboxylic acid groups, this PIP-TMC based membrane exhibits rejection selectivity for divalent ($MgSO_4$) salt ions [46].

5.1.2. Effect of pH in the feed of filtration test

Table 5: List of PIP-TMC membranes and their preparation condition for different pH feed

Sample name	Aqueous solution (S1) % w/v	Organic solution (S2) % w/v	Immersing time in S1	Drying at room temperature	Immersing time in S2	Curing
PT2-B	PIP 2% + TEA 4 % + NaOH 1%	TMC 0.45 %	180 s	150 s	180 s	600 s at 100 °C
PT2-C	PIP 2% + TEA 4 % + NaOH 1%	TMC 0.45 %	180 s	150 s	180 s	600 s at 100 °C
PT2-D	PIP 2% + TEA 4 % + NaOH 1%	TMC 0.45 %	180 s	150 s	180 s	600 s at 100 °C

Table 6: Comparison of flux and rejection of feeds with different pH on PIP-TMC membranes

Sample name	Flux of distilled water (L/m ² h)	Flux of salt feed (L/m ² h)	Rejection (%)	pH of salt feed
PT2-B	28	16	19.18	2
PT2-C	27.33	14.66	74.18	6
PT2-D	28	12.66	86.87	9.5

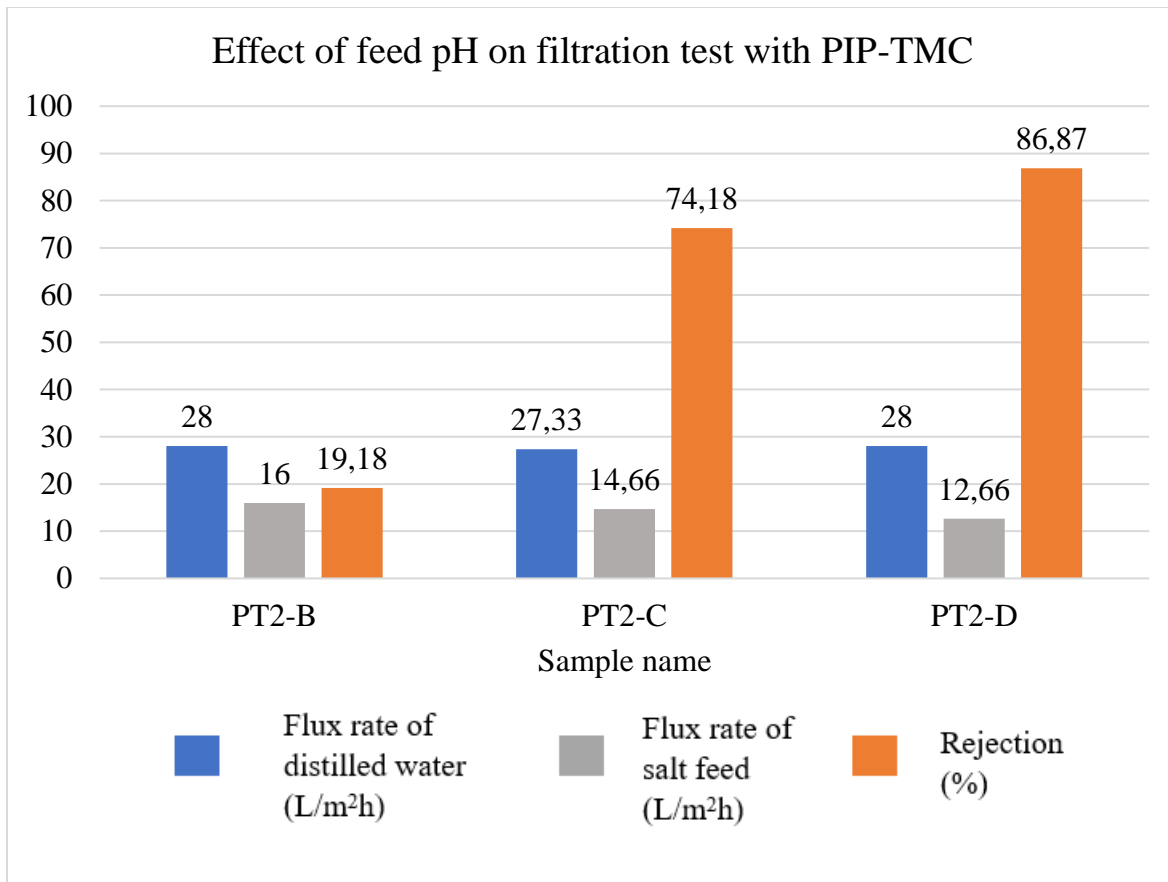


Figure 18: Graph of flux and rejection on different pH feed with PIP-TMC membranes

Table 5 shows the preparation condition of samples prepared to test with feed solutions of different pH, and the results are shown in Table 6 and compared in the graph from Figure 18. The sample that gave 97% rejection (PT2) earlier is replicated but could not get the same level of rejection with the usual feed (MgSO_4 with 2000 ppm), and it decreased to 74 % rejection, resulting in a greater flux rate. It is believed that this might be due to exposure TMC to environment every time during the experiment because when the TMC container opened newly it give high rejection and it started to decrease time to time for the same preparation parameters.

Then, the feed solution pH was decreased by adding HCL, which resulted in an increase in conductivity from 2448 $\mu\text{S}/\text{cm}$ (MgSO_4 with 2000 ppm) to 6100 $\mu\text{S}/\text{cm}$. Feed with low pH-2 gives very low rejection, 19.18%, and a very low increase in flux.

However, when the feed's pH was increased to 9.5 by adding NaOH, no difference in conductivity was noticed in the feed solution. The result was an increase in rejection and also an increase in flux rate. The leading causes of PIP-TMC membranes' greater rejection of MgSO_4 at high pH levels and lower rejection at low pH levels might be due to the variations in the membrane's surface charge, the Donnan exclusion effect, solute speciation, and the membrane's structural makeup. Higher pH causes the membrane to become more negatively charged, which improves rejection and sulfate ion electrostatic repulsion. On the other hand, lower pH results in lower rejection rates due to the decreased membrane charge and possible structural alterations [8, 47].

5.1.3. Double testing on one sample:

Table 7: The best sample of PIP-TMC was chosen for double testing and its preparation condition.

Sample name	Aqueous solution (S1) % w/v	Organic solution (S2) % w/v	Immersing time in S1	Drying at room temperature	Immersing time in S2	Curing
PT2-E	PIP 2% + TEA 4 % + NaOH 1%	TMC 0.45 %	180 s	150 s	180 s	600 s at 100 °C

Table 8: comparison flux and rejection of chosen for double testing.

Sample name	Test.no	Flux of distilled water (L/m ² h)	Flux of salt feed (L/m ² h)	Rejection (%)
PT2-E	1	20	10	90.55
	2	80	15.68	75

A membrane with 0.45% (w/v) concentration of TMC gives out the best ion salt rejection and is subjected to double testing. Table 7 gives the preparation parameters replicated from Sample PT2. In the fresh membrane, rejection was 90.55%, and the test was repeated after washing the membrane mildly in distilled water to remove the salt and stabilizing it with the distilled water in the beginning.

The rejection of the second test decreased to 75 % with an increase in flux rate, which is depicted in Table 8 and compared in the graph mentioned in Figure 19. The decrease of rejection and increase of flux can be caused by increase of pore size resulted by flow of ions through the pore during the first test or the sensitive membrane might be damaged during cleaning process. During the second test, the flux was very high at the beginning of the filtration test and decreased over time. It might be caused by fouling and it shows that the fouling is inevitable in dead-end filtration method.

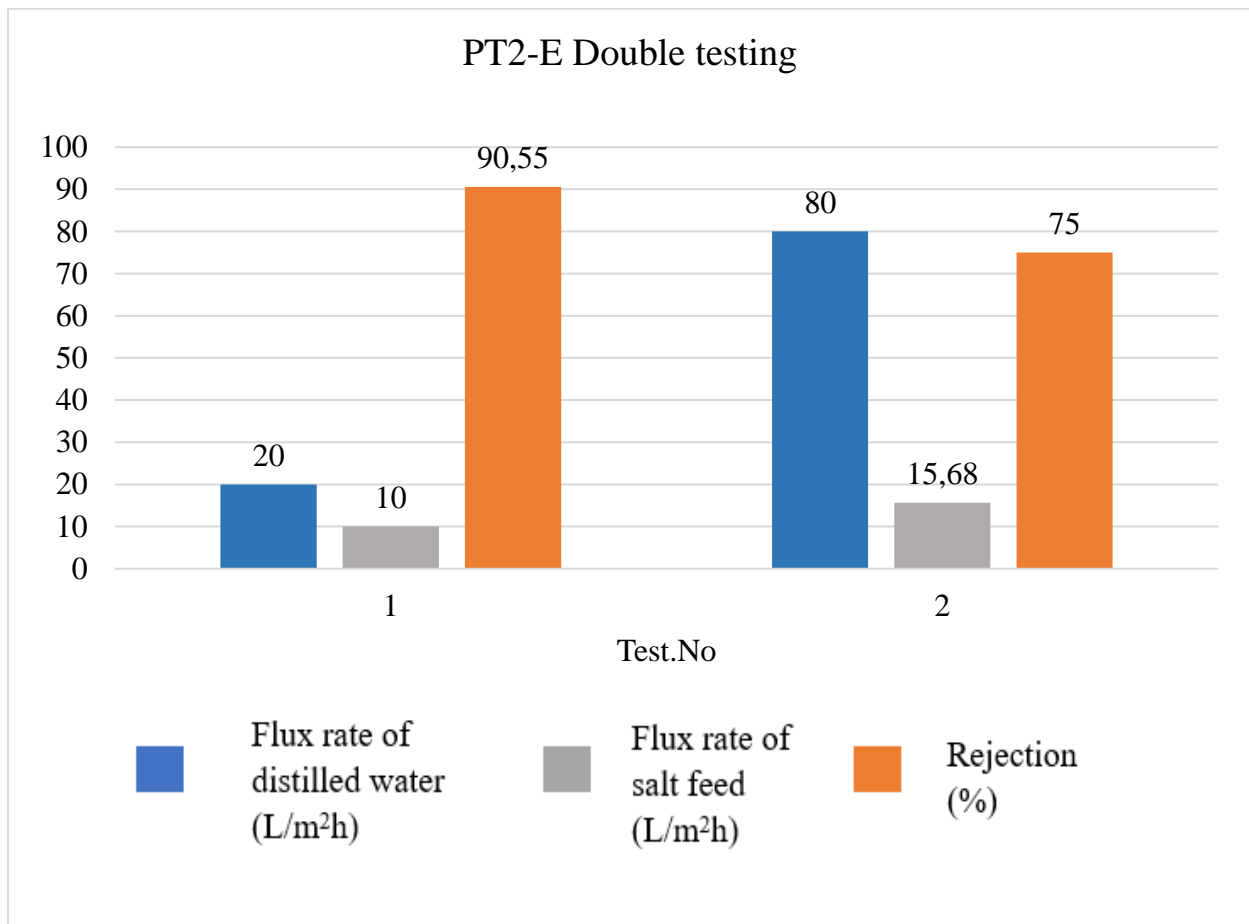


Figure 19: Graph of flux and rejection of chosen sample for double testing

5.1.4. Surface morphology analysis:

Table 9: list of PIP-TMC membranes for SEM analysis

Sample name	Aqueous solution (S1) % w/v	Organic solution (S2) % w/v	Immersing time in S1	Drying at room temperature	Immersing time in S2	Curing
PT1	PIP 2% + TEA 4 % + NaOH 1%	TMC 0.2 %	180 s	150 s	180 s	600 s at 100 °C
PT2	PIP 2% + TEA 4 % + NaOH 1%	TMC 0.45 %	180 s	150 s	180 s	600 s at 100 °C
PT3	PIP 2% + TEA 4 % + NaOH 1%	TMC 0.2 %	180 s	150 s	180 s	Dried at room temperature

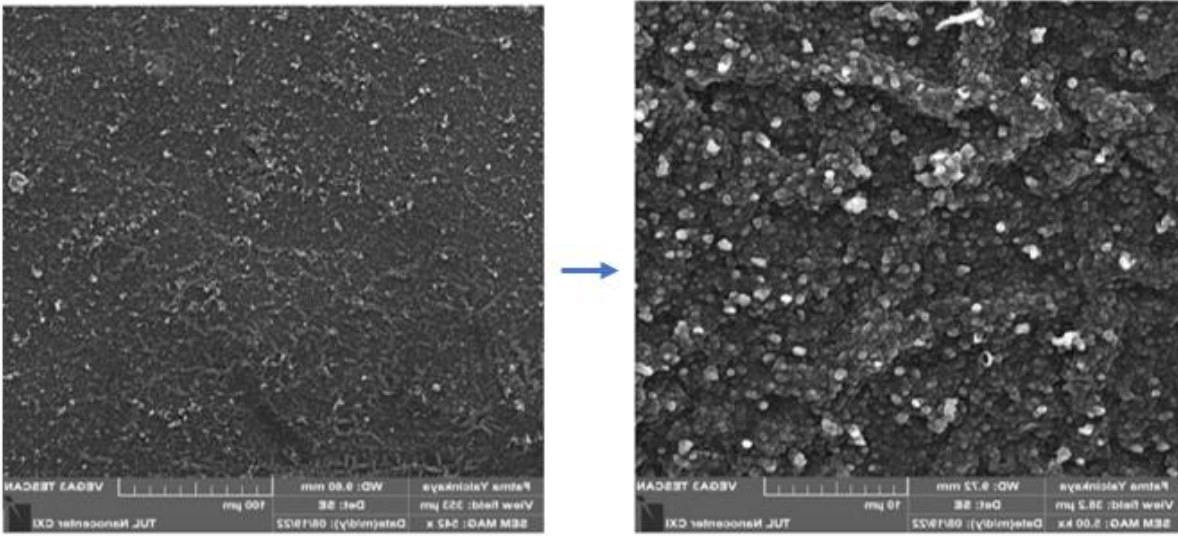


Figure 20: SEM images of PT1.

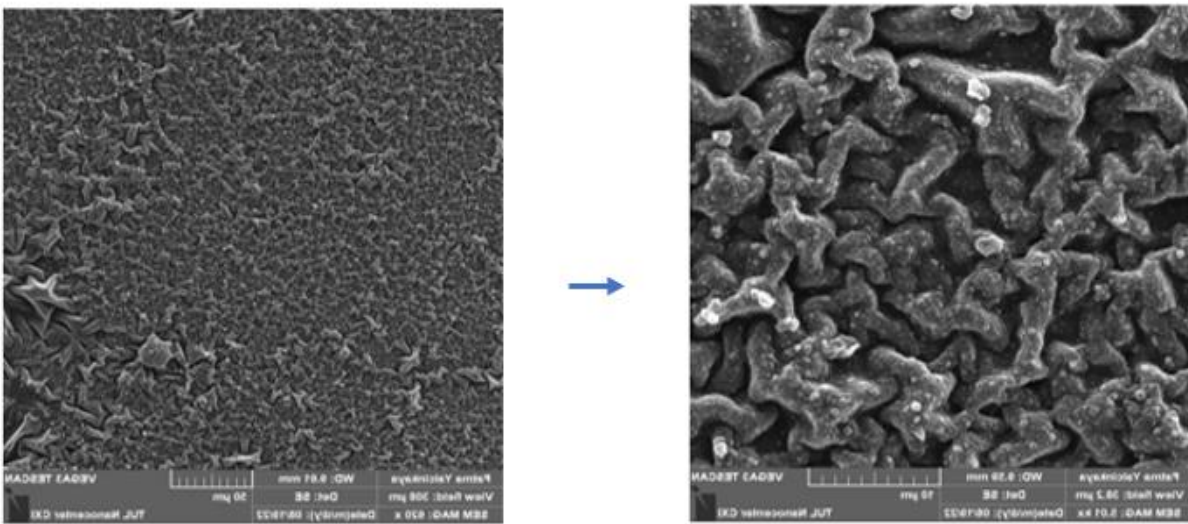


Figure 21: SEM images of PT2.

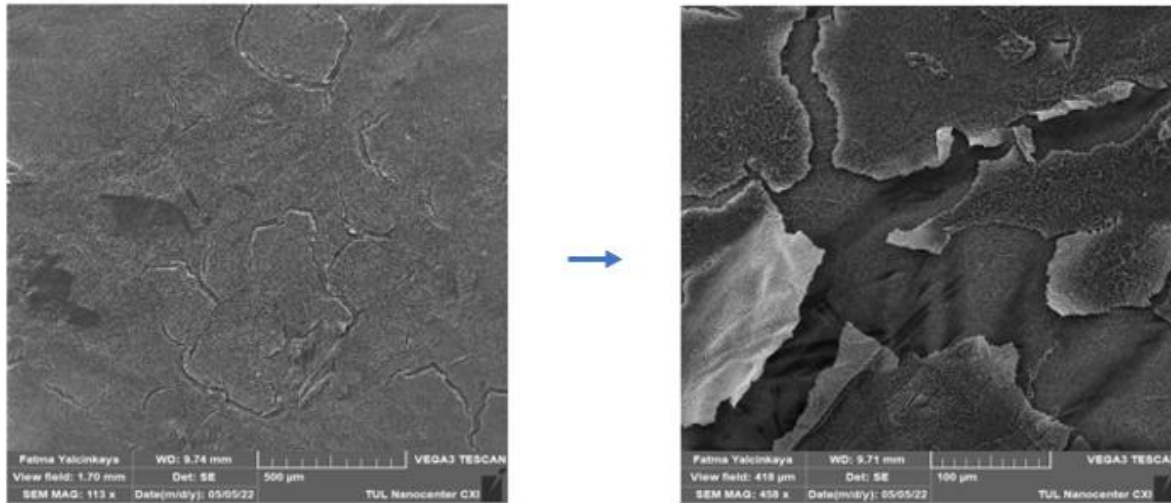


Figure 22: SEM images of PT3.

Table 9 displays the sample preparation parameters that have been used for surface morphology analysis. SEM images of the sample shows the surface morphology of the membrane and observed that the thin-film layer is successfully formed. Images of PT1 (Figure 20) show the presence of a thin-film layer on the surface without any visible cracks. Figure 21, in which the SEM images PT2 were displayed, shows a high level of surface roughness when compared to PT1. The SEM images of sample PT1 and PT2 matches with filtration performance by giving information that the increase of concentration of TMC gives out dense and thick layer which was the reason for increase of rejection and decrease of flux when TMC concentration is increased. Figure 22 displays the open cracks throughout the surface of the membrane sample PT3. Images of PT3 show that the curing process after the preparation is mandatory for crosslinking.

5.1.5. Contact angle:

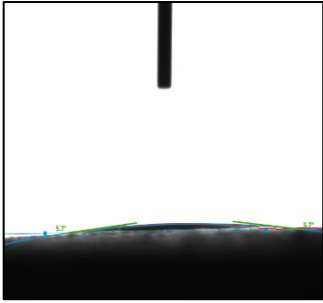
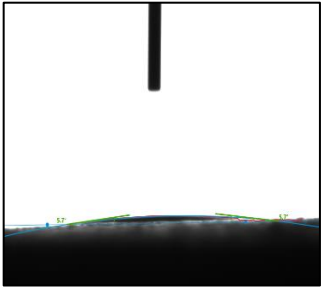
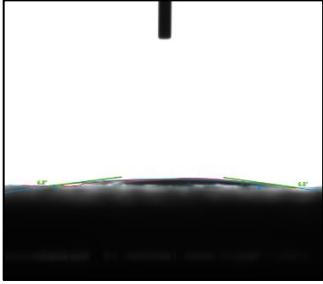
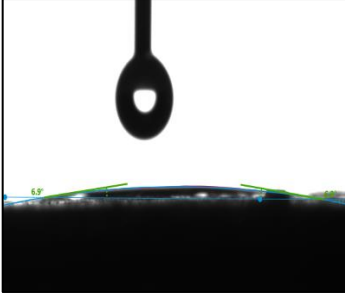
Table 10: PIP-TMC sample list and preparation condition for contact angle measurement.

Sample name	Aqueous solution (S1) % w/v	Organic solution (S2) % w/v	Immersing time in S1	Drying at room temperature	Immersing time in S2	Curing
PT2-F	PIP 2% + TEA 4% + NaOH 1%	TMC 0.45 %	180 s	150 s	180 s	600 s at 100 °C
PT2-G	PIP 2% + TEA 4% + NaOH 1%	TMC 0.45 %	180 s	150 s	180 s	600 s at 100 °C
PT2-H	PIP 2% + TEA 4% + NaOH 1%	TMC 0.45 %	180 s	150 s	180 s	600 s at 100 °C
PT2-I	PIP 2% + TEA 4% + NaOH 1%	TMC 0.45 %	180 s	150 s	180 s	600 s at 100 °C

Table 11: Average contact angle of PIP-TMC sample in different solution.

Sample name	Average contact angle	Temperature	Type of feed
PT2-F	5.9 °	22.8 °C	Distilled water
PT2-G	6.1 °	22.4 °C	MgSO ₄ with pH-2
PT2-H	6.6 °	22.2 °C	MgSO ₄
PT2-I	6.8 °	22.3 °C	MgSO ₄ with pH-9.5

Table 12: Contact angle images of PIP-TMC membranes.

Sample name	Images of contact angle
PT2-F	
PT2-G	
PT2-H	
PT2-I	

The sample that gave high rejection (PT2) was chosen for the contact angle measurement. Table 10 gives the sample details of preparation. The contact angle of four solutions was measured, and mean values are depicted in Table 11, all measurements were taken at room temperature, and three measurements were taken to determine the mean value. It has been understood that the PIP-TMC membrane has a good hydrophilic nature with all types of feed solutions. Table 12 displays the images of contact angle measurement on the prepared sample. PIP-TMC membranes are hydrophilic because they contain hydrophilic functional groups like amines and amides, have a high surface energy, and have a surface morphology that facilitates water interaction. These features improve the water permeability of the membrane [47].

5.1.6. Chemical Composition Analysis:

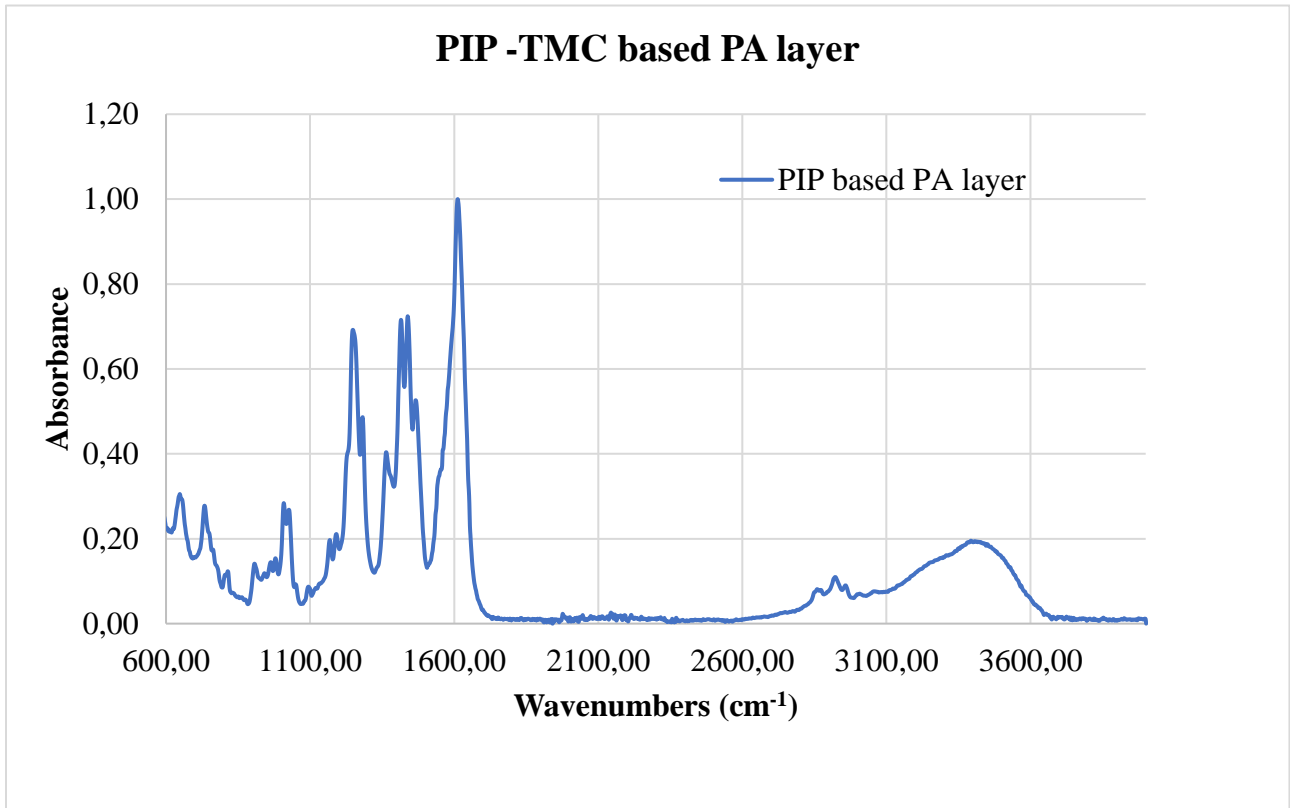


Figure 23: FT-IR of PIP-TMC based PA membrane.

For FT-IR analysis, the PIP-TMC thin-film was prepared without the nanofibrous and nonwoven composite support. Figure 23 shows the analyzed spectra of the PIP-TMC-based thin-film membrane. The amide I band typically appears in the range of 1600-1700 cm^{-1} and is primarily associated with the stretching vibrations of (C=O) carbonyl bonds in the amide groups (-CONH-) of the polyamide structure. From Figure 23, the peak appeared around 1650-1670 cm^{-1} , Showing the polyamide formed by polymerization between the PIP and TMC. In the spectrum of PIP and TMC polymerization, the peak appeared s around 1550-1570 cm^{-1} showing the presence of N-H bending and C-N stretching vibrations in the amide groups. This confirms the PA layer formed By PIP and TMC [8, 48].

5.2. Results and discussion of filtration test and characterization of MPD-TMC membrane:

5.2.1. Filtration test:

Table 13: List of MPD-TMC membranes and their preparation condition.

Sample name	Aqueous solution (S1) % w/v	Organic solution (S2) % w/v	Immersing time in S1	Drying at room temperature	Immersing time in S2	Curing
MT1	MPD 2% + TEA 2 % + SDS 0.2%	TMC 0.2 %	180 s	150 s	180 s	600 s at 100 °C
MT2	MPD 2% + TEA 2 % + SDS 0.2%	TMC 0.3 %	180 s	150 s	180 s	600 s at 100 °C
MT3	MPD 2% + TEA 2 % + SDS 0.2%	TMC 0.45 %	180 s	150 s	180 s	600 s at 100 °C
MT4	MPD 2% + TEA 2 % + SDS 0.2%	TMC 0.6 %	180 s	150 s	180 s	600 s at 100 °C

It was very difficult to get a good range of rejection and flux rates with MPD-TMC membranes. After a few experiments, the results are promising in terms of rejection with monovalent salt (NaCl) but with a very low range of flux. Table 13 contains the preparation parameters of MPD-TMC membranes for evaluation. The flux and rejection rate of MPD-TMC samples are portrayed in Table 14. The increase of TMC concentration gives out the increase in rejection rate and a decrease of flux until a certain point this might be due to, the active barrier layer of MPD-based membranes was more compact and denser and presence the aromatic amine structure, the membranes demonstrated rejection selectivity for monovalent (NaCl) salt ions [46]. Figure 24 gives a graphical comparison of the performance of prepared MPD-TMC samples with different

concentrations of TMC. A high rejection of 74% was obtained with a 0.45% (w/v) TMC concentration and a very low flux rate of 0.42 (L/m²h).

Table 14: Comparison of flux and rejection of MPD-TMC membranes

Sample name	Flux of distilled water (L/m ² h)	type of salt feed	Flux of salt feed (L/m ² h)	Rejection (%)
MT1	60	NaCl	5.33	10
MT2	33.33	NaCl	1.77	36
MT3	40	NaCl	0.42	74
MT4	16	NaCl	1	29

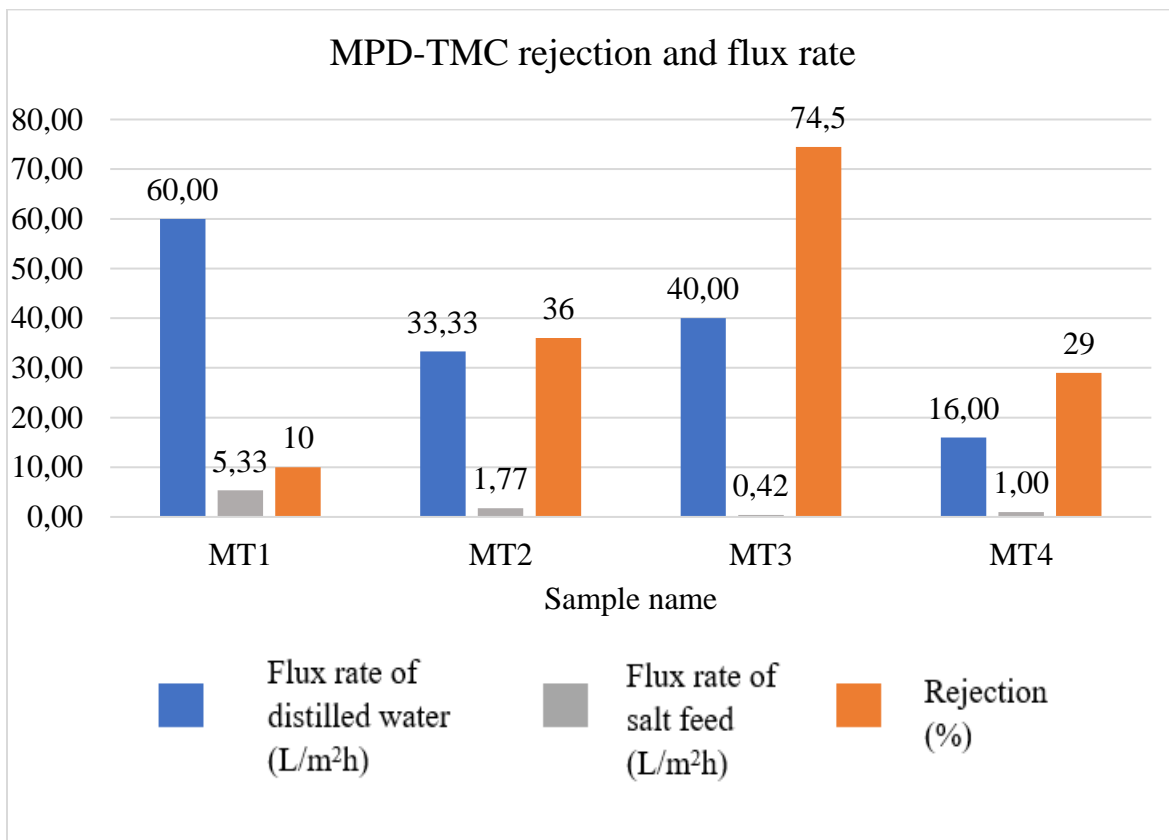


Figure 24: Graph of flux and rejection of MPD-TMC membranes.

5.2.2. Effect of pH in the feed of filtration test:

Table 15: List of MPD-TMC membranes and their preparation condition for different pH feed.

Sample name	Aqueous solution (S1) % w/v	Organic solution (S2) % w/v	Immersing time in S1	Drying at room temperature	Immersing time in S2	Curing
MT3-A	MPD 2% + TEA 2 % + SDS 0.2%	TMC 0.45 %	180 s	150 s	180 s	600 s at 100 °C
MT3-B	MPD 2% + TEA 2 % + SDS 0.2%	TMC 0.45 %	180 s	150 s	180 s	600 s at 100 °C
MT3-C	MPD 2% + TEA 2 % + SDS 0.2%	TMC 0.45 %	180 s	150 s	180 s	600 s at 100 °C

Table 16: Comparison of flux and rejection of feeds with different pH on MPD-TMC membranes.

Sample name	Flux of distilled water (L/m ² h)	Flux of salt feed (L/m ² h)	Rejection (%)	pH of salt feed
MT3-A	35	2.3	12	2
MT3-B	33	0.38	65	6
MT3-C	40	0.40	72	9.5

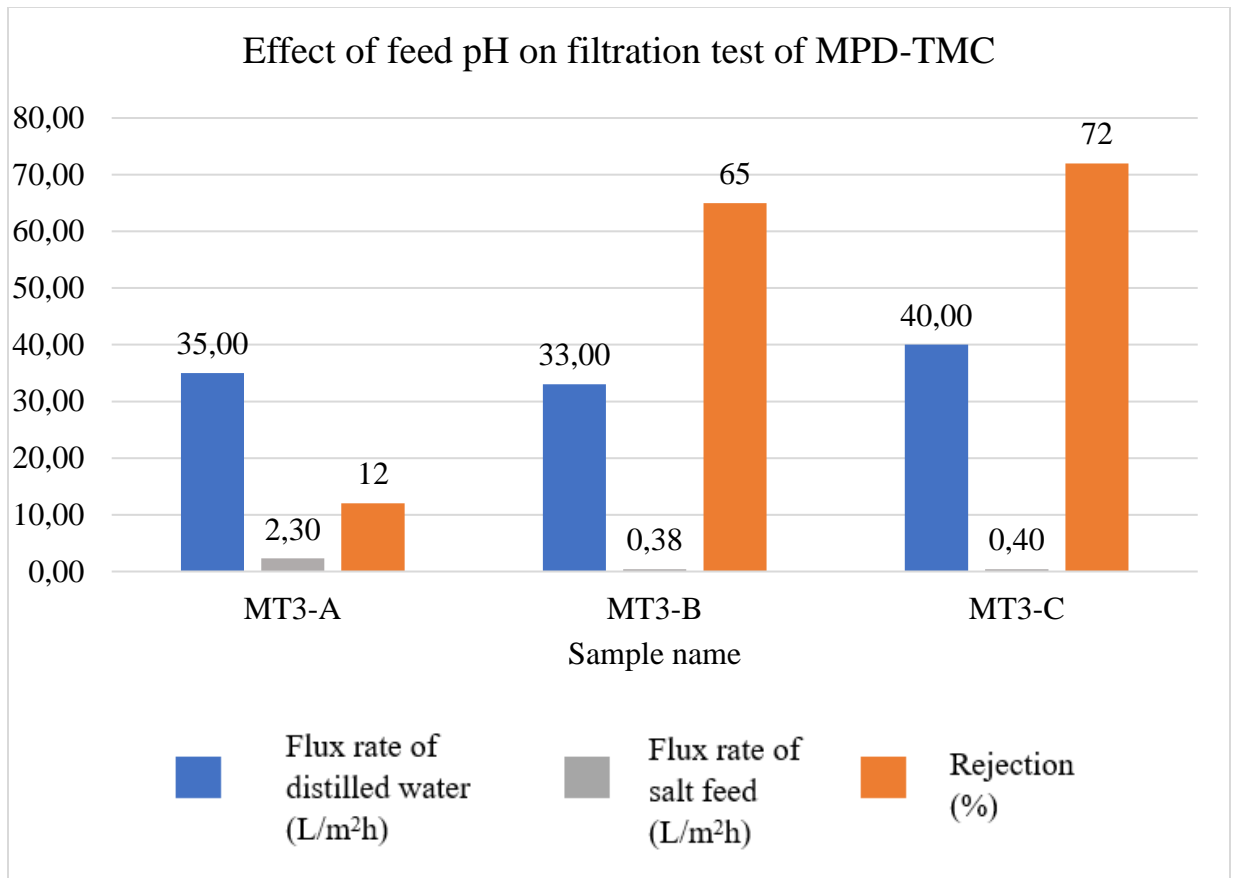


Figure 25: Graph of flux and rejection on Different pH feed with MPD-TMC membranes.

Table 15 gives the details of the preparation parameter of the MPD-TMC membrane, which is the replication of sample MT3. Similar to the PIP-TMC membrane, the MPD-TMC membrane also showed an increase in rejection with an increase in the feed pH. Table 16 gives out the rejection and flux rates of feeds with different pH levels. One of the important observations from the test is that the increase in pH increases rejection in promising levels with also a very low-level increase in the flux rate. This variation in flux might be because of similar mechanism in PIP-TMC membranes that the MPD-TMC membranes' greater rejection of NaCl at high pH levels and decreased rejection at low pH levels are variations in the membrane's surface charge, the Donnan exclusion effect, solute speciation, and the membrane's structural makeup. A higher pH causes the membrane to become more negatively charged, which improves rejection and increases the electrostatic repulsion of chloride (Cl⁻) ions. On the other hand, lower pH results in lower rejection rates due to the decreased membrane charge and possible structural alterations [8, 47].

5.2.3. Surface morphology analysis:

Table 17: List of MPD-TMC membranes for SEM analysis.

Sample name	Aqueous solution (S1) % w/v	Organic solution (S2) % w/v	Immersing time in S1	Drying at room temperature	Immersing time in S2	Curing
MT1-S	MPD 2% + TEA 2 % + SDS 0.2%	TMC 0.2 %	180 s	150 s	180 s	600 s at 100 °C
MT2-S	MPD 2% + TEA 2 % + SDS 0.2%	TMC 0.3 %	180 s	150 s	180 s	600 s at 100 °C
MT3-S	MPD 2% + TEA 2 % + SDS 0.2%	TMC 0.45 %	180 s	150 s	180 s	600 s at 100 °C
MT4-S	MPD 2% + TEA 2 % + SDS 0.2%	TMC 0.6 %	180 s	150 s	180 s	600 s at 100 °C

Table 17 lists the samples subjected to SEM analysis and the preparation parameters we described in the table.

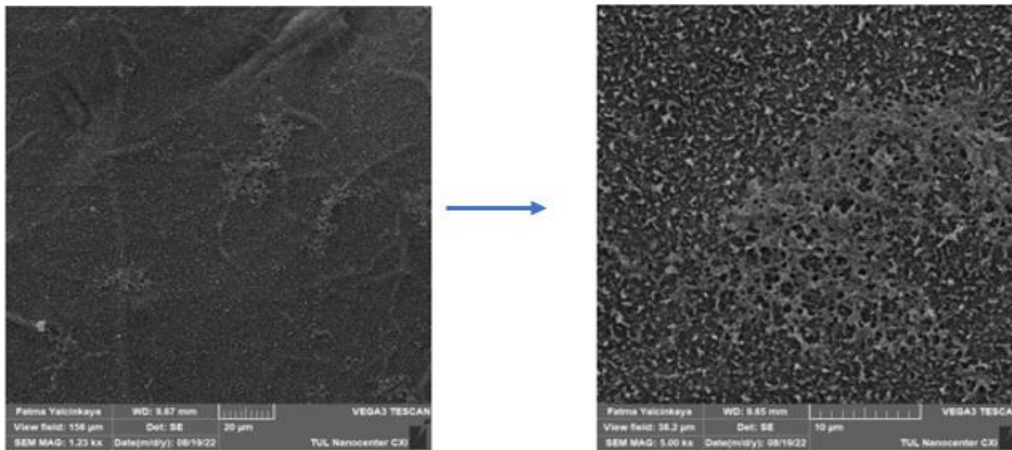


Figure 26: SEM images of MT1-S

Figure 26 shows the SEM image of sample MT1-S. It shows the rough surface of the MPD-TMC membrane and accumulation in some spots of the sample, but no cracks are visible. It is visible that the dense layer formed all over the surface of the composite support.

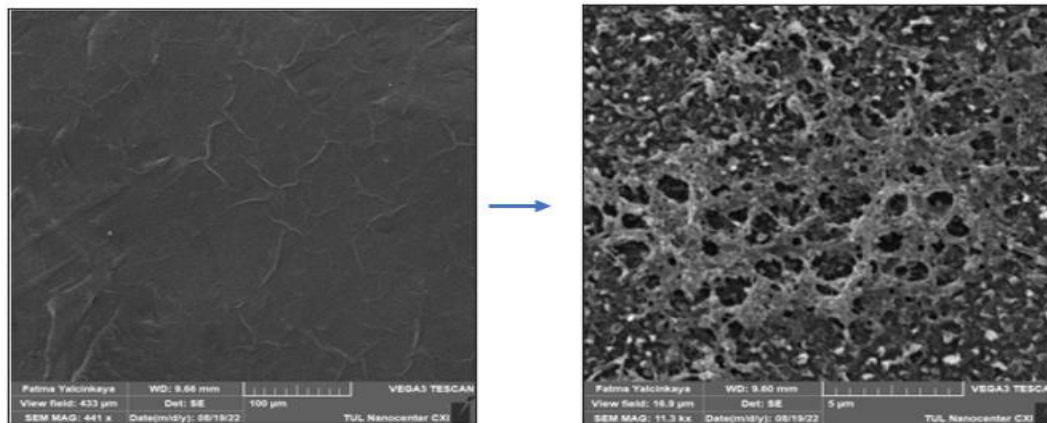


Figure 27: SEM images of MT2-S.

Sample MT2-S SEM images displayed in Figure 27 show a dense layer of the membrane was formed with more accumulations than the MT1-S.

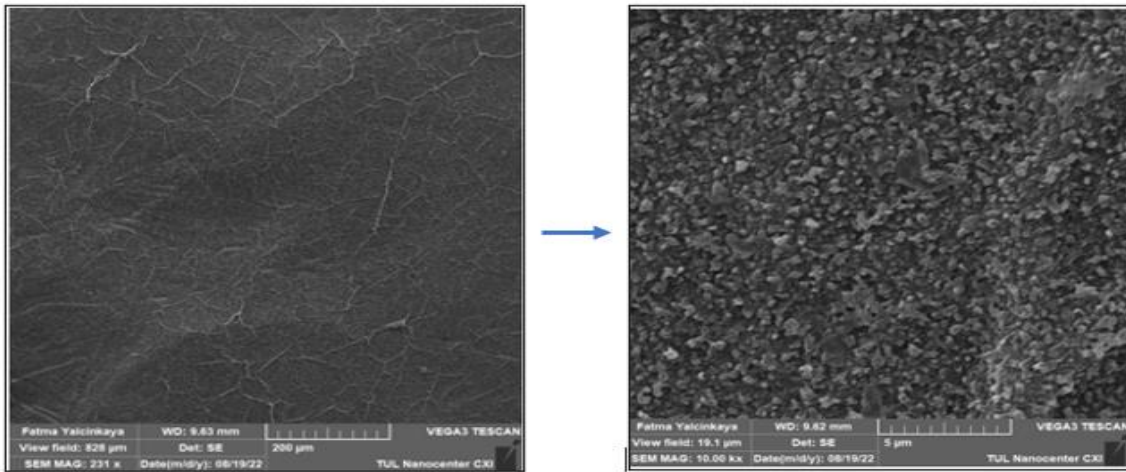


Figure 28: SEM images of MT3-S.

Sample MT3-S surface analysis through SEM shown in Figure 28 concludes that a clear image of an even surface compared to other MPD-TMC membranes and a dense layer without any cracks on the surface is clearly visible through the SEM images.

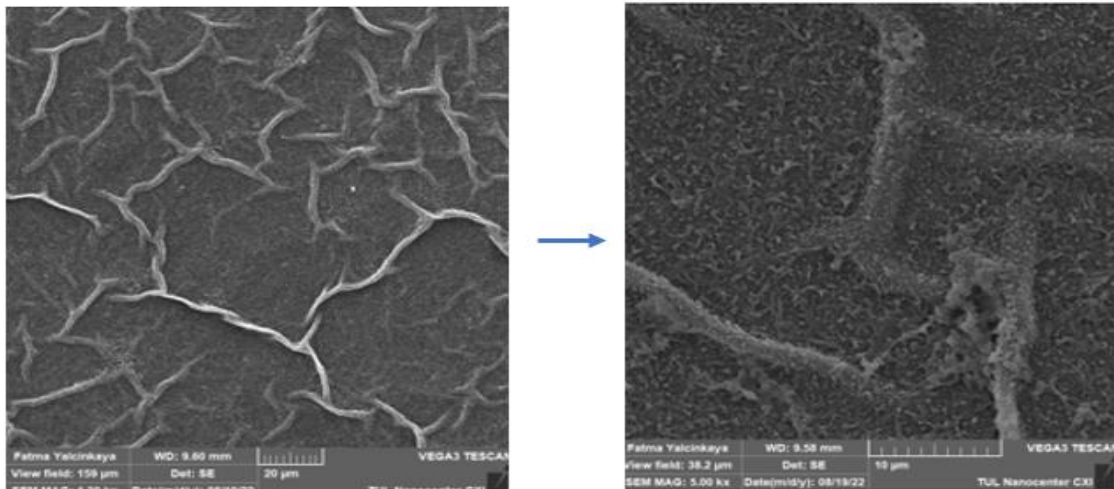


Figure 29: SEM images of MT4-S.

SEM images of sample MT4-S displayed in Figure 29 show that the highest concentration of TMC, 0.6 % (w/v), shows the membrane's very dense and uneven structure. However, no visible cracks were observed, and these results match the low flux rate of the filtration tests.

5.2.4. Contact angle:

Table 18: MPD-TMC sample list and preparation condition for contact angle measurement.

Sample name	Aqueous solution (S1) % w/v	Organic solution (S2) % w/v	Immersing time in S1	Drying at room temperature	Immersing time in S2	Curing
MT3-D	MPD 2% + TEA 2% + SDS 0.2%	TMC 0.45 %	180 s	150 s	180 s	600 s at 100 °C
MT3-E	MPD 2% + TEA 2% + SDS 0.2%	TMC 0.45 %	180 s	150 s	180 s	600 s at 100 °C
MT3-F	MPD 2% + TEA 2% + SDS 0.2%	TMC 0.45 %	180 s	150 s	180 s	600 s at 100 °C
MT3-G	MPD 2% + TEA 2% + SDS 0.2%	TMC 0.45 %	180 s	150 s	180 s	600 s at 100 °C

Table 19: Average contact angle of MPD-TMC sample in different solution.

Sample name	Average contact angle	Temperature	Type of feed
MT3-D	70.89 °	22.8 °C	Distilled water
MT3-E	69.87 °	22.8 °C	NaCl with pH-2
MT3-F	76.72 °	22.8 °C	NaCl
MT3-G	65.29 °	22.8 °C	NaCl with pH-9.5

Table 20: images of contact angle measurement on MPD-TMC membranes.

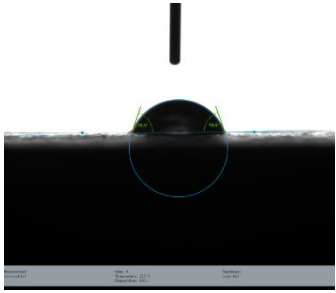

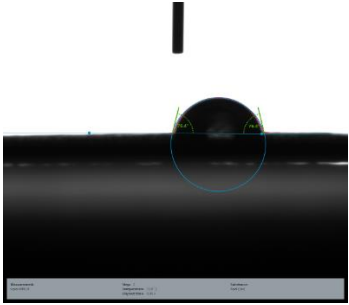
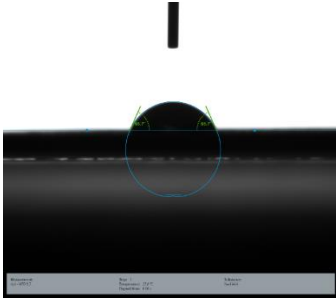
Sample name	Images of contact angle
MT3-D	
MT3-E	
MT3-F	
MT3-G	

Table 18 gives the preparation parameter of samples prepared for contact angle measurement which is the replication of sample MT3. The results of MPD-TMC membranes' contact angle measurement shown in Table 19 coincide with the flux rate of the filtration test. All solutions show a contact angle below 90 °, which means the sample is hydrophilic in nature. All measurements were taken at room temperature, and with each type of feed solution, three measurements were taken to get the mean value. Table 20 displays the images of the contact angle with the MPD-TMC membrane with all four kinds of feed solution. The hydrophobic nature of aromatic rings in MPD and the presence of fewer hydrophilic functional groups compared to PIP may be the cause of the lower hydrophilicity of MPD-TMC membranes. This concludes the effect of higher water contact angles compared to PIP-TMC membranes [47].

5.2.5. Chemical Composition Analysis:

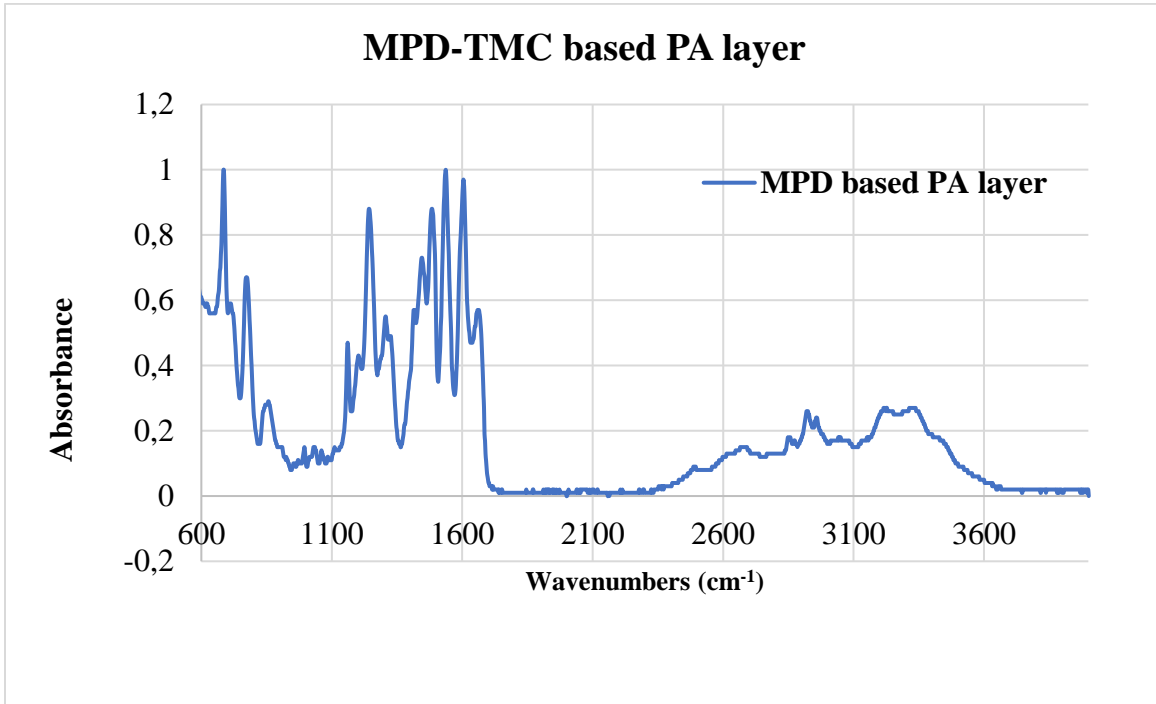


Figure 30: FT-IR of MPD-TMC based PA membrane.

Figure 30 shows the spectrum of the FT-IR chemical composition analysis of the prepared MPD-TMC thin-film layer. For FT-IR characterization, the MPD-TMC based polyamide layer is prepared separately without using the composite support. Broad and intense peaks between 1650 and 1700 cm^{-1} indicate the presence of amide bonds ($\text{C}=\text{O}$) and show that successful polymerization has occurred. The peaks between 1500 and 1650 cm^{-1} show that the characteristic peak of polyamides is the N-H bending vibration. Aromatic C-H stretching vibrations were observed in the range of 3000-3100 cm^{-1} . This shows the successful formation of the MPD-TMC-based PA membrane [8, 48].

6. CONCLUSION:

This thesis has investigated various aspects of membrane technology, focusing on the fabrication and optimization of thin-film composite (TFC) membranes using PIP, MPD, and TMC as key monomers. Several significant discoveries have been made through theoretical discussions and experimental investigations, contributing to the understanding and advancement of membrane-based filtration processes. The results of the filtration tests demonstrate the efficacy of the fabricated TFNC membranes in separating salt ions from feed solutions. Furthermore, the concentration of monomers was found to play a pivotal role in determining the properties of the membranes. The PIP-TMC membrane, with a TMC concentration of 0.45% (w/v), demonstrated promising results in the separation of divalent salts (MgSO_4), with a rejection rate of up to 97% and a flux rate of 8.6 L/ m² h. Furthermore, the MPD-TMC-based membrane exhibited the highest rejection rate of 74% for monovalent salts (NaCl) with a low flux rate of 0.42 L/m² h.

Additionally, the impact of pH variations in the feedwater on membrane performance was investigated. An increase in pH level on the feed solution resulted in an increased rejection rate with a slight variation in flux rate for both the MPD-TMC and PIP-TMC membranes. Surface morphology analysis and contact angle measurements provided insights into the membrane's structural and surface properties. In contrast, chemical composition analysis confirmed the presence of the desired functional groups necessary to prove the polyamide layer formed by IP between PIP/MPD with TMC. In conclusion, the optimization study to enhance the TFC membrane's performance for saltwater filtration has yielded significant findings and advancements. Several pivotal conclusions have been reached after meticulous testing and analysis.

Furthermore, both the MPD-TMC and PIP-TMC based membranes show increased rejection with increased pH value of feed. Further research is needed, mainly on pH, to determine the effect of pH on feed solution and the cause of flux change and rejection rate. The cross-flow filtration method must be carried out to understand filtration efficiency better. Furthermore, research on using different support materials is needed to know the effect of support materials on filtration efficiency and fouling properties of the membrane.

7. REFERENCE:

- [1] ANON., 2023. *Water*. *Wikipedia [online]* [vid. 17. prosinec 2023]. Získáno z: <https://en.wikipedia.org/wiki/Water> .
- [2] EKE, Joyner, Ahmed YUSUF, Adewale GIWA a Ahmed SODIQ. The global status of desalination: An assessment of current desalination technologies, plants and capacity. *Desalination* [online]. 2020, **495**, 114633 [vid. 2024-05-16]. ISSN 0011-9164. Dostupné z: doi:10.1016/J.DESAL.2020.114633
- [3] ALKLAIBI, A. M. a Noam LIOR. Membrane-distillation desalination: Status and potential. *Desalination* [online]. 2005, **171**(2), 111–131 [vid. 2024-05-16]. ISSN 00119164. Dostupné z: doi:10.1016/j.desal.2004.03.024
- [4] JONES, Edward, Manzoor QADIR, Michelle T.H. VAN VLIET, Vladimir SMAKHTIN a Seong mu KANG. The state of desalination and brine production: A global outlook. *Science of the Total Environment* [online]. 2019, **657**, 1343–1356 [vid. 2024-05-16]. ISSN 18791026. Dostupné z: doi:10.1016/j.scitotenv.2018.12.076
- [5] *Basic Principles of Membrane Technology - Marcel Mulder - Google Books* [online]. [vid. 2024-05-06]. Dostupné z: https://books.google.lv/books?id=SP2_GYvL384C&printsec=frontcover#v=onepage&q&f=false
- [6] ULBRICHT, Mathias. Advanced functional polymer membranes. *Polymer* [online]. 2006, **47**(7), 2217–2262 [vid. 2024-05-05]. ISSN 0032-3861. Dostupné z: doi:10.1016/J.POLYMER.2006.01.084
- [7] Chapter 1 Overview membrane technology. *Membrane Science and Technology* [online]. 2004, **10**(C), 1–23 [vid. 2024-05-12]. ISSN 09275193. Dostupné z: doi:10.1016/S0927-5193(04)80018-4

- [8] BAKER, Richard W. Membrane Technology and Applications. *Membrane Technology and Applications* [online]. 2012 [vid. 2024-05-12]. Dostupné z: doi:10.1002/9781118359686
- [9] PEINEMANN, Klaus Viktor a Suzana Pereira NUNES. Membrane Technology. *Membrane Technology* [online]. 2010, 4 [vid. 2024-05-12]. Dostupné z: doi:10.1002/9783527631407
- [10] *Basic Principles of Membrane Technology - Marcel Mulder - Google Books* [online]. [vid. 2024-05-12]. Dostupné z: https://books.google.lv/books/about/Basic_Principles_of_Membrane_Technology.html?id=y2_wCAAQBAJ&redir_esc=y
- [11] ZAHID, Muhammad, Anum RASHID, Saba AKRAM, Zulfiqar Ahmad REHAN a Wasif RAZZAQ. A Comprehensive Review on Polymeric Nano-Composite Membranes for Water Treatment. *Journal of Membrane Science & Technology* [online]. 2018, 08(01) [vid. 2024-05-12]. Dostupné z: doi:10.4172/2155-9589.1000179
- [12] GOH, Pei Sean, Tuck Whye WONG, Jun Wei LIM, Ahmad Fauzi ISMAIL a Nidal HILAL. Innovative and sustainable membrane technology for wastewater treatment and desalination application. *Innovation Strategies in Environmental Science* [online]. 2020, 291–319 [vid. 2024-05-11]. Dostupné z: doi:10.1016/B978-0-12-817382-4.00009-5
- [13] NATH. MEMBRANE SEPARATION PROCESSES. [online]. 2018 [vid. 2024-05-13]. Dostupné z: https://books.google.com/books/about/MEMBRANE_SEPARATION_PROCESSES.html?id=1VrWDQAAQBAJ
- [14] ASAD, Asad, Dan SAMEOTO a Mohtada SADRZADEH. Overview of membrane technology. *Nanocomposite Membranes for Water and Gas Separation* [online]. 2020, 1–28 [vid. 2024-05-07]. Dostupné z: doi:10.1016/B978-0-12-816710-6.00001-8
- [15] MULDER, M. MEMBRANE PREPARATION | Phase Inversion Membranes. *Encyclopedia of Separation Science* [online]. 2000, 3331–3346 [vid. 2024-05-13]. Dostupné z: doi:10.1016/B0-12-226770-2/05271-6

- [16] Membrane and Desalination Technologies. *Membrane and Desalination Technologies* [online]. 2011 [vid. 2024-05-13]. Dostupné z: doi:10.1007/978-1-59745-278-6
- [17] LALIA, Boor Singh, Victor KOCHKODAN, Raed HASHAIKEH a Nidal HILAL. A review on membrane fabrication: Structure, properties and performance relationship. *Desalination* [online]. 2013, **326**, 77–95 [vid. 2024-05-13]. ISSN 0011-9164. Dostupné z: doi:10.1016/J.DESAL.2013.06.016
- [18] APEL, P. Track etching technique in membrane technology. *Radiation Measurements* [online]. 2001, **34**(1–6), 559–566 [vid. 2024-05-13]. ISSN 1350-4487. Dostupné z: doi:10.1016/S1350-4487(01)00228-1
- [19] HOOVER, Laura A., Jessica D. SCHIFFMAN a Menachem ELIMELECH. Nanofibers in thin-film composite membrane support layers: Enabling expanded application of forward and pressure retarded osmosis. *Desalination* [online]. 2013, **308**, 73–81 [vid. 2024-05-13]. ISSN 00119164. Dostupné z: doi:10.1016/J.DESAL.2012.07.019
- [20] *Surface modification by plasma polymerization and application of plasma polymers as biomaterials* / [online]. [vid. 2024-05-13]. Dostupné z: https://www.researchgate.net/publication/35659526_Surface_modification_by_plasma_polymerization_and_application_of_plasma_polymers_as_biomaterials
- [21] ZOU, L., I. VIDALIS, D. STEELE, A. MICHELMORE, S. P. LOW a J. Q.J.C. VERBERK. Surface hydrophilic modification of RO membranes by plasma polymerization for low organic fouling. *Journal of Membrane Science* [online]. 2011, **369**(1–2), 420–428 [vid. 2024-05-13]. ISSN 0376-7388. Dostupné z: doi:10.1016/J.MEMSCI.2010.12.023
- [22] ZHU, Shu, Song ZHAO, Zhi WANG, Xinxia TIAN, Mengqi SHI, Jixiao WANG a Shichang WANG. Improved performance of polyamide thin-film composite nanofiltration membrane by using polyetersulfone/polyaniline membrane as the substrate. *Journal of Membrane Science* [online]. 2015, **493**, 263–274 [vid. 2024-05-18]. ISSN 0376-7388. Dostupné z: doi:10.1016/J.MEMSCI.2015.07.013

- [23] JIMENEZ SOLOMON, Maria Fernanda, Yogesh BHOLE a Andrew Guy LIVINGSTON. High flux membranes for organic solvent nanofiltration (OSN)—Interfacial polymerization with solvent activation. *Journal of Membrane Science* [online]. 2012, **423–424**, 371–382 [vid. 2024-05-18]. ISSN 0376-7388. Dostupné z: doi:10.1016/J.MEMSCI.2012.08.030
- [24] MORGAN, Paul W. a Stephanie L. KWOLEK. Interfacial polycondensation. II. Fundamentals of polymer formation at liquid interfaces. *Journal of Polymer Science* [online]. 1959, **40(137)**, 299–327 [vid. 2024-05-13]. ISSN 1542-6238. Dostupné z: doi:10.1002/POL.1959.1204013702
- [25] KHORSHIDI, Behnam, Thomas THUNDAT, David PERNITSKY a Mohtada SADRZADEH. A parametric study on the synergistic impacts of chemical additives on permeation properties of thin film composite polyamide membrane. *Journal of Membrane Science* [online]. 2017, **535**, 248–257 [vid. 2024-05-13]. ISSN 18733123. Dostupné z: doi:10.1016/J.MEMSCI.2017.04.052
- [26] LAU, W. J., A. F. ISMAIL, N. MISDAN a M. A. KASSIM. A recent progress in thin film composite membrane: A review. *Desalination* [online]. 2012, **287**, 190–199 [vid. 2024-05-13]. ISSN 00119164. Dostupné z: doi:10.1016/J.DESAL.2011.04.004
- [27] CADOTTE, J. E., R. J. PETERSEN, R. E. LARSON a E. E. ERICKSON. A new thin-film composite seawater reverse osmosis membrane. *Desalination* [online]. 1980, **32(C)**, 25–31 [vid. 2024-05-13]. ISSN 0011-9164. Dostupné z: doi:10.1016/S0011-9164(00)86003-8
- [28] LIN, Lin, Rene LOPEZ, Guy Z. RAMON a Orlando CORONELL. Investigating the void structure of the polyamide active layers of thin-film composite membranes. *Journal of Membrane Science* [online]. 2016, **497**, 365–376 [vid. 2024-05-08]. ISSN 0376-7388. Dostupné z: doi:10.1016/J.MEMSCI.2015.09.020
- [29] LI, Xuesong, Qing LI, Wangxi FANG, Rong WANG a William B. KRANTZ. Effects of the support on the characteristics and permselectivity of thin film composite membranes. *Journal of Membrane Science* [online]. 2019, **580**, 12–23 [vid. 2024-05-13]. ISSN 0376-7388. Dostupné z: doi:10.1016/J.MEMSCI.2019.03.003

- [30] KHORSHIDI, Behnam, Javad HAJINASIRI, Guibin MA, Subir BHATTACHARJEE a Mohtada SADRZADEH. Thermally resistant and electrically conductive PES/ITO nanocomposite membrane. *Journal of Membrane Science* [online]. 2016, **500**, 151–160 [vid. 2024-05-13]. ISSN 0376-7388. Dostupné z: doi:10.1016/J.MEMSCI.2015.11.015
- [31] LIN, Lin, Rene LOPEZ, Guy Z. RAMON a Orlando CORONELL. Investigating the void structure of the polyamide active layers of thin-film composite membranes. *Journal of Membrane Science* [online]. 2016, **497**, 365–376 [vid. 2024-05-13]. ISSN 0376-7388. Dostupné z: doi:10.1016/J.MEMSCI.2015.09.020
- [32] KHAN, Anwar Ul Haq, Zafarullah KHAN a Isam H. ALJUNDI. Improved hydrophilicity and anti-fouling properties of polyamide TFN membrane comprising carbide derived carbon. *Desalination* [online]. 2017, **420**, 125–135 [vid. 2024-05-16]. ISSN 00119164. Dostupné z: doi:10.1016/J.DESAL.2017.07.002
- [33] PEEVA, Polina Dobromirova, Nina MILLION a Mathias ULBRICHT. Factors affecting the sieving behavior of anti-fouling thin-layer cross-linked hydrogel polyethersulfone composite ultrafiltration membranes. *Journal of Membrane Science* [online]. 2012, **390–391**, 99–112 [vid. 2024-05-16]. ISSN 0376-7388. Dostupné z: doi:10.1016/J.MEMSCI.2011.11.025
- [34] SANDERS, David F., Zachary P. SMITH, Ruilan GUO, Lloyd M. ROBESON, James E. MCGRATH, Donald R. PAUL a Benny D. FREEMAN. Energy-efficient polymeric gas separation membranes for a sustainable future: A review. *Polymer* [online]. 2013, **54**(18), 4729–4761 [vid. 2024-05-13]. ISSN 0032-3861. Dostupné z: doi:10.1016/J.POLYMER.2013.05.075
- [35] (PDF) *Membrane Technology for Water Treatment Applications* [online]. [vid. 2024-05-13]. Dostupné z: https://www.researchgate.net/publication/301647575_Membrane_Technology_for_Water_Treatment_Applications

- [36] BASILE, Angelo (Angelo Bruno) a S. P. (Suzana Pereira) NUNES. Advanced membrane science and technology for sustainable energy and environmental applications. nedatováno.
- [37] ABID, Monis Bin, Roswanira Abdul WAHAB, Mohamed Abdel SALAM, Lassaad GZARA a Iqbal Ahmed MOUJDIN. Desalination technologies, membrane distillation, and electrospinning, an overview. *Heliyon* [online]. 2023, **9**(2), e12810 [vid. 2024-05-16]. ISSN 2405-8440. Dostupné z: doi:10.1016/J.HELIYON.2023.E12810
- [38] KIM, C. K., J. H. KIM, I. J. ROH a J. J. KIM. The changes of membrane performance with polyamide molecular structure in the reverse osmosis process. *Journal of Membrane Science* [online]. 2000, **165**(2), 189–199 [vid. 2024-05-14]. ISSN 0376-7388. Dostupné z: doi:10.1016/S0376-7388(99)00232-X
- [39] MANSOURPANAH, Y., S. S. MADAENI a A. RAHIMPOUR. Fabrication and development of interfacial polymerized thin-film composite nanofiltration membrane using different surfactants in organic phase; study of morphology and performance. *Journal of Membrane Science* [online]. 2009, **343**(1–2), 219–228 [vid. 2024-05-14]. ISSN 0376-7388. Dostupné z: doi:10.1016/J.MEMSCI.2009.07.033
- [40] YUNG, Lewis, Hongyang MA, Xiao WANG, Kyunghwan YOON, Ran WANG, Benjamin S. HSIAO a Benjamin CHU. Fabrication of thin-film nanofibrous composite membranes by interfacial polymerization using ionic liquids as additives. *Journal of Membrane Science* [online]. 2010, **365**(1–2), 52–58 [vid. 2024-05-14]. ISSN 03767388. Dostupné z: doi:10.1016/J.MEMSCI.2010.08.033
- [41] GHOSH, Asim K., Byeong Heon JEONG, Xiaofei HUANG a Eric M.V. HOEK. Impacts of reaction and curing conditions on polyamide composite reverse osmosis membrane properties. *Journal of Membrane Science* [online]. 2008, **311**(1–2), 34–45 [vid. 2024-05-14]. ISSN 03767388. Dostupné z: doi:10.1016/J.MEMSCI.2007.11.038
- [42] JIN, Ying a Zhaohui SU. Effects of polymerization conditions on hydrophilic groups in aromatic polyamide thin films. *Journal of Membrane Science* [online]. 2009, **330**(1–2),

- 175–179 [vid. 2024-05-14]. ISSN 03767388. Dostupné z: doi:10.1016/J.MEMSCI.2008.12.055
- [43] HIROSE, Masahiko, Hiroki ITO a Yoshiyasu KAMIYAMA. Effect of skin layer surface structures on the flux behaviour of RO membranes. *Journal of Membrane Science* [online]. 1996, **121**(2), 209–215 [vid. 2024-05-14]. ISSN 0376-7388. Dostupné z: doi:10.1016/S0376-7388(96)00181-0
- [44] YALCINKAYA, Baturalp, Fatma YALCINKAYA a Jiri CHALOUPEK. Optimisation of thin film composite nanofiltration membranes based on laminated nanofibrous and nonwoven supporting material. *Desalination and Water Treatment* [online]. 2017, **59**, 19–30 [vid. 2024-05-16]. ISSN 19443986. Dostupné z: doi:10.5004/DWT.2016.0254
- [45] PETERSEN, Robert J. Composite reverse osmosis and nanofiltration membranes. *Journal of Membrane Science* [online]. 1993, **83**(1), 81–150 [vid. 2024-05-20]. ISSN 0376-7388. Dostupné z: doi:10.1016/0376-7388(93)80014-O
- [46] YALCINKAYA, Baturalp, Fatma YALCINKAYA a Jiri CHALOUPEK. Optimisation of thin film composite nanofiltration membranes based on laminated nanofibrous and nonwoven supporting material. *Desalination and Water Treatment* [online]. 2017, **59**, 19–30 [vid. 2024-05-20]. ISSN 19443986. Dostupné z: doi:10.5004/DWT.2016.0254
- [47] CADOTTE, J. E., R. S. KING, R. J. MAJERLE a R. J. PETERSEN. Interfacial Synthesis in the Preparation of Reverse Osmosis Membranes. *Journal of Macromolecular Science, Part A* [online]. 1981, **15**(5), 727–755 [vid. 2024-05-20]. ISSN 0022233X. Dostupné z: doi:10.1080/00222338108056764
- [48] *Spectrometric Identification of Organic Compounds, 7th Edition - Robert M. Silverstein, Francis X. Webster, David Kiemle - Google Books* [online]. [vid. 2024-05-16]. Dostupné z: https://books.google.cz/books/about/Spectrometric_Identification_of_Organic.html?id=mQ8cAAAAQBAJ&redir_esc=y